

Article

Three Nimesulide Derivatives: Synthesis, Ab-initio Structure Determination from Powder X-ray Diffraction and Quantitative Analysis of Molecular Surface Electrostatic Potential

Tanusri Dey, Paramita Chatterjee, Abir Bhattacharya, Sarbani Pal, and Alok K Mukherjee

Cryst. Growth Des., **Just Accepted Manuscript** • DOI: 10.1021/acs.cgd.5b01547 • Publication Date (Web): 25 Jan 2016

Downloaded from <http://pubs.acs.org> on January 27, 2016

Just Accepted

“Just Accepted” manuscripts have been peer-reviewed and accepted for publication. They are posted online prior to technical editing, formatting for publication and author proofing. The American Chemical Society provides “Just Accepted” as a free service to the research community to expedite the dissemination of scientific material as soon as possible after acceptance. “Just Accepted” manuscripts appear in full in PDF format accompanied by an HTML abstract. “Just Accepted” manuscripts have been fully peer reviewed, but should not be considered the official version of record. They are accessible to all readers and citable by the Digital Object Identifier (DOI®). “Just Accepted” is an optional service offered to authors. Therefore, the “Just Accepted” Web site may not include all articles that will be published in the journal. After a manuscript is technically edited and formatted, it will be removed from the “Just Accepted” Web site and published as an ASAP article. Note that technical editing may introduce minor changes to the manuscript text and/or graphics which could affect content, and all legal disclaimers and ethical guidelines that apply to the journal pertain. ACS cannot be held responsible for errors or consequences arising from the use of information contained in these “Just Accepted” manuscripts.



Three Nimesulide Derivatives: Synthesis, Ab-initio Structure Determination from Powder X-ray Diffraction and Quantitative Analysis of Molecular Surface Electrostatic Potential

Tanusri Dey^a, Paramita Chatterjee^{a,b}, Abir Bhattacharya^c, Sarbani Pal^d and Alok K. Mukherjee^{a,*}

^a Department of Physics, Jadavpur University, Jadavpur, Kolkata-700032, India.

^b Department of Physics, Lady Brabourne College, Kolkata-700017, India.

^c Department of Physics, Amity University, Kolkata-700156, India.

^d Department of Chemistry, MNR Degree and PG College, Kukatpally, Hyderabad-500072, India.

Abstract

Three nimesulide derivatives, N-[4-(2,5-dioxo-pyrrolidin-1-yl)-2-phenoxyphenyl]methanesulfonamide (**2**), N-[4-(4-methanesulfonylamino-3-phenoxy phenylsulfamoyl) phenyl]acetamide (**3**) and 4-(4-methanesulfonylamino-3-phenoxyphenyl-carbamoyl)-butanoic acid (**4**), have been synthesized and their crystal structures have been determined from laboratory powder X-ray diffraction data. The nature of intermolecular interactions in **2-4** has been analyzed through Hirshfeld surfaces and 2D fingerprint plots, and compared with that in the nimesulide polymorphs (**1a** and **1b**). The crystal packing in **2-4** exhibits an interplay of N-H...O, O-H...O (in **4**), C-H...O and C-H... π (in **2**) hydrogen bonds, which assemble molecules into supramolecular framework. Hydrogen-bond based interactions in **2-4** have been complemented by calculating molecular electrostatic potential (MEP) surfaces. In a competitive molecular recognition situation, the effectiveness of -NH moiety as hydrogen bond donor is comparable to that of -COOH moiety in **4**. Hirshfeld surface analyses of **2-4** as well as a few related nimesulide derivatives indicate that about 90% of the Hirshfeld surface areas in these compounds are due to H...H, C...H and O...H contacts.

Corresponding author

Alok K. Mukherjee

Department of Physics, Jadavpur University, Jadavpur, Kolkata-700032, India.

E-mail: akm_ju@rediffmail.com, Phone No. +919331041417, Fax: 033 24138917

Three Nimesulide Derivatives: Synthesis, Ab-initio Structure Determination from Powder X-ray Diffraction and Quantitative Analysis of Molecular Surface Electrostatic Potential

Tanusri Dey^a, Paramita Chatterjee^{a,b}, Abir Bhattacharya^c, Sarbani Pal^d and Alok K. Mukherjee^{a,*}

^a Department of Physics, Jadavpur University, Jadavpur, Kolkata-700032, India.

^b Department of Physics, Lady Brabourne College, Kolkata-700017, India.

^c Department of Physics, Amity University, Kolkata-700156, India.

^d Department of Chemistry, MNR Degree and PG College, Kukatpally, Hyderabad-500072, India.

E-mail: akm_ju@rediffmail.com

Abstract

Three nimesulide derivatives, N-[4-(2,5-dioxo-pyrrolidin-1-yl)-2-phenoxyphenyl]methanesulfonamide (**2**), N-[4-(4-methanesulfonylamino-3-phenoxy phenylsulfamoyl) phenyl]acetamide (**3**) and 4-(4-methanesulfonylamino-3-phenoxyphenyl-carbamoyl)-butanoic acid (**4**), have been synthesized and their crystal structures have been determined from laboratory powder X-ray diffraction data. The nature of intermolecular interactions in **2-4** has been analyzed through Hirshfeld surfaces and 2D fingerprint plots, and compared with that in the nimesulide polymorphs (**1a** and **1b**). The crystal packing in **2-4** exhibits an interplay of N-H...O, O-H...O (in **4**), C-H...O and C-H... π (in **2**) hydrogen bonds, which assemble molecules into supramolecular framework. Hydrogen-bond based interactions in **2-4** have been complemented by calculating molecular electrostatic potential (MEP) surfaces. In a competitive molecular recognition situation, the effectiveness of -NH moiety as hydrogen bond donor is comparable to that of -COOH moiety in **4**. Hirshfeld surface analyses of **2-4** as well as a few related nimesulide derivatives indicate that about 90% of the Hirshfeld surface areas in these compounds are due to H...H, C...H and O...H contacts.

Introduction

Intermolecular interactions, in particular, hydrogen bonds have been a topic of considerable importance across many scientific disciplines¹⁻³, and it is indeed the basis of life due to its structural role, in DNA^{2, 4, 5}, enzymes⁶⁻⁸ and proteins⁹⁻¹¹. In crystal engineering perspective, hydrogen bonds play a key role for the assembly and organization of organic building blocks using the concept of motifs and synthons^{12, 13}. In pharmaceutical science, the active pharmaceutical ingredients (APIs), which enable the efficacy of drug delivery system, are inherently amenable to crystal engineering as they contain functional groups with multiple hydrogen bond donors and acceptors¹⁴⁻¹⁷. Many of the synthons involving N/O-H...O/N hydrogen bonds possess the requisite robustness and reproducibility for the design and synthesis of new solid-state materials with desirable structure and properties^{18, 19}. In addition to relatively strong hydrogen bonds, weak interactions such as C-H...X (X=O, N), C/N-H... π hydrogen bonds and π ... π stacking also influence significantly the self-assembly process in organic compounds. These interactions are individually weaker and geometrically less well-defined, their combined effect, however, can be equally important as strong interactions^{20, 21}. The distance and directional criteria of specific hydrogen bonds made by the functional groups in molecules have been generally used in describing the crystal packing of molecular solids²²⁻²⁴.

Etter^{25, 26} developed a set of empirical rules useful for determining preferred modes of hydrogen bonding. However, most hydrogen bonds are primarily electrostatic in nature and vary in strength according to the different donor/acceptor properties of functional groups and their environment, thus predicting supramolecular structures driven by hydrogen bonding can be challenging²⁷⁻³⁰. In this context, effective means for ranking hydrogen-bond donor and acceptor groups could provide useful guidelines for designing new materials. Hunter and co-workers^{31, 32} proposed a strategy for ranking the relative strength of hydrogen-bond donors and acceptors based on molecular electrostatic potential (MEP) surface value. An extensive body of work correlating MEP with crystal packing via intermolecular interactions has been reported³³⁻³⁷.

In general, knowledge of crystal structure is a prerequisite for understanding intermolecular interactions and other properties of crystalline materials. Although single crystal X-ray diffraction (XRD) is the method of choice for determining crystal structures of molecular compounds, an intrinsic limitation of this approach is the requirement to obtain single crystal of

1
2
3 appropriate size and quality that make them amenable to structure analysis. As many important
4 materials including the present nimesulide derivatives are available only as microcrystalline
5 powder, structure determination directly from powder X-ray diffraction (PXRD) is highly
6 desirable. The task of crystal structure determination from X-ray powder diffraction is, however,
7 considerably more challenging than that of its single crystal counterpart³⁸ because, first, the
8 information content of a powder diffraction is markedly lower and second, it is far more difficult
9 to extract structural information from a PXRD pattern due to systematic as well as random
10 overlapping of peaks. Fortunately, there have been significant advances in recent years in the
11 techniques for carrying out ab-initio structure determination of organic molecular solids directly
12 from PXRD data, particularly through the development of the direct-space strategy for structure
13 solution³⁹⁻⁴⁵.

24 Nimesulide, N-(4-nitro-2-phenoxyphenyl) methanesulfonamide (**1**), is a well known non-
25 steroidal anti-inflammatory drug (NSAID), which can inhibit cyclooxygenase-2 (COX-2)
26 enzyme selectively⁴⁶. Since the nitro group in **1** is known to be associated with toxic side effects
27 including gastrointestinal erosions⁴⁷⁻⁴⁹, several nimesulide derivatives aiming at improving its
28 tolerability profile and reducing its toxicity have been reported by changing in **1** the nitro group
29 with an appropriate electron withdrawing moiety⁴⁹⁻⁵¹. With this background, we synthesized
30 three nimesulide derivatives, N-[4-(2,5-dioxo-pyrrolidin-1-yl)-2-phenoxyphenyl]
31 methanesulfonamide (**2**), N-[4-(4-methanesulfonylamino-3-phenoxy phenylsulfamoyl) phenyl]
32 acetamide (**3**) and 4-(4-methanesulfonylamino-3-phenoxyphenyl-carbamoyl)-butanoic acid (**4**),
33 with different aromatic/aliphatic substitutions replacing the nitro group in nimesulide (**1**) to
34 analyze differences in crystal packing due to changes in the substituents. Since our attempts to
35 grow suitable single crystals of **2-4** for X-ray analysis resulted in assemblies of microcrystals,
36 structure determination was attempted from X-ray powder diffraction. Intermolecular hydrogen
37 bonds facilitating supramolecular structures in **2-4** have been discussed with a detailed
38 assessment of molecular electrostatic potential (MEP) surface for ranking different hydrogen
39 bond donor and acceptor groups. An investigation of close intermolecular interactions in **2-4**,
40 nimesulide (**1**) and a few related substituted nimesulide derivatives via Hirshfeld surface analysis
41 is also presented.
42
43
44
45
46
47
48
49
50
51
52
53
54
55
56
57
58
59
60

Experimental Section

Materials and general methods

All chemicals were obtained from commercial sources and used without further purification. Solvents were dried using the standard method, and chromatographic purification was performed using silica gel (100-200 mesh). Elemental analysis was carried out with a PerkinElmer 240 C analyzer. Fourier transform infrared (FTIR) spectra were recorded on a Perkin Elmer Spectrum Bx II Spectrometer as KBr pellets. ^1H NMR and ^{13}C NMR were measured at 22° C using a Bruker DPX-300 Spectrometer using CDCl_3 or DMSO-d_6 as solvent. Mass spectra were recorded on a Jeol JMC D-300 instrument with an electron ionization potential of 70 eV. Melting points were determined by an open glass capillary method and were uncorrected.

Synthesis

N-(4-amino-2-phenoxy phenyl) methanesulfonamide (**1'**) was prepared by reduction of N-(4-nitro-2-phenoxy phenyl) methanesulfonamide (**1**, nimesulide) using Sn and HCl. The reaction was carried out at 90° C for 3 hours (Scheme 1). For the synthesis of **2** and **4**, the aromatic amine (**1'**) (278 mg, 1.0 mmol) was treated with the corresponding cyclic anhydrides, **2a** (148 mg, 1.0 mmol) and **4a** (100 mg, 1.0 mmol), according to the desired product followed by refluxing in glacial acetic acid (3 ml) for 1 hour in presence of anhydrous sodium acetate (Scheme 1). After completion of reaction (monitored by TLC at regular intervals), the reaction mixture was quenched in crushed ice and stirred. The solid mass separated was filtered and dried. The crude product on purification by column chromatography on silica gel (100-200 mesh) using chloroform-ethyl acetate (3:1) and crystallization from aqueous methanol (1:1) yielded microcrystalline powders of N-[4-(2,5-dioxo-pyrrolidin-1-yl)-2-phenoxyphenyl]methanesulfonamide (**2**) and 4-(4-methanesulfonylamino-3-phenoxyphenyl-carbamoyl)-butanoic acid (**4**). For synthesis of **3**, amine (**1'**) (1g, 3.56 mmol) was dissolved in dry chloroform and triethylamine (0.6 ml) was added to it. The solution was cooled to 0° C and sulfonyl chloride (**3a**, 3.56 mmol) was added drop wise with stirring. The reaction mixture was further stirred for 15 minutes, poured into water (20 ml) and extracted with chloroform (3×25 ml). Organic layer was collected and washed with 10% HCl (10ml) followed by water (2×10 ml), dried over anhydrous Na_2SO_4 and concentrated. The residue was crystallized from

chloroform-ethyl acetate (3:1) to yield microcrystalline powder of N-[4-(4-methanesulfonylamino-3-phenoxy phenylsulfamoyl) phenyl] acetamide (**3**).

N-[4-(2,5-dioxo-pyrrolidin-1-yl)-2-phenoxyphenyl]methanesulfonamide (2)

Colorless solid; mp 226(2) °C; IR (KBr) $\nu_{\max}/\text{cm}^{-1}$: 1707; ^1H NMR (300 MHz, CDCl_3) δ 2.7 (s, 4H), 3.1 (s, 3H), 6.8 (s, 1H), 7.1 (m, 3H), 7.3 (m, 1H), 7.4 (m, 3H), 9.5 (s, NH); ^{13}C NMR (75 MHz, CDCl_3) δ 28.3 (CH₂), 39.8 (CH₃), 115.9 (CH), 119.1 (CH), 120.8 (CH), 122.1 (CH), 124.8 (CH), 128.1 (C), 128.6 (C), 130.2 (CH), 147.2 (C), 155.1 (C), 175.7 (CO); Mass 361 (M⁺, 100%); Elemental analysis found: C 56.70, H 4.50, N 7.74%; calculated for C₁₇H₁₆O₅N₂S; C 56.66, H 4.47, N 7.77%.

N-[4-(4-methanesulfonylamino-3-phenoxy phenylsulfamoyl) phenyl] acetamide (3)

Colorless solid; mp 185(2) °C; IR (KBr) $\nu_{\max}/\text{cm}^{-1}$: 3231, 3315, 1658, 1604; ^1H NMR (200 MHz, DMSO-*d*₆) δ 9.87 (s, 1H), 9.77 (s, 1H), 8.17 (s, 1H), 6.74-7.78 (m, 12H), 2.16 (s, 3H), 2.89 (s, 3H), 9.77 (s, 1H), Mass 476 (M⁺, 100%); Elemental analysis found: C 53.18, H 4.25, N, 8.95%; calculated for C₂₁H₂₁O₆N₃S₂; C 53.04, H 4.45, N 8.84%.

4-(4-methanesulfonylamino-3-phenoxyphenyl-carbamoyl)-butanoic acid (4)

Colorless solid; mp 127(1) °C; IR (KBr) $\nu_{\max}/\text{cm}^{-1}$: 1671; ^1H NMR (400 MHz, DMSO-*d*₆) δ 1.7 (m, 2H), 2.4 (m, 4H), 3.0 (s, 3H), 7.0 (dd, *J* 8.8 and 1 Hz, 2H), 7.2-7.3 (m, 4H), 7.42 (m, 2H), 10.0 (1H, NH); ^{13}C NMR (75 MHz, DMSO-*d*₆) δ 20.2 (CH₂), 32.9 (CH₂), 35.3 (CH₂), 108.6 (CH), 113.8 (CH), 119.1 (CH), 122.3 (C), 123.8 (CH), 127.8 (CH), 129.9 (CH), 138.3 (C), 151.0 (C), 155.9 (C), 170.7 (C), 174.0 (CO); Mass 391 (M⁺, 100%); Elemental analysis found: C 55.21, H 4.95, N 7.32 %; calculated for C₁₈H₂₀O₆N₂S; C 55.10, H 5.10, N 7.14%.

X-ray Powder Diffraction

Powder X-ray diffraction (PXRD) data of **2-4** were recorded at ambient temperature [293 (2) K] on a Bruker D8 Advance diffractometer operating in the Bragg-Brentano geometry with CuK α radiation ($\lambda=1.5418\text{\AA}$) for **2** and **4**, and Ge-monochromated CuK α_1 radiation ($\lambda=1.5406\text{\AA}$) for **3**. The PXRD patterns of **2-4** were indexed using the NTREOR code⁵² in the program EXPO 2014⁵³ yielding monoclinic unit cells. Given the volume of unit cell and consideration of density, the number of formula units in the unit cell of **2-4** turned out as Z=4. Although the correct space group could not be assigned unambiguously on the basis of systematic absences, statistical

1
2
3 analysis of PXRD data using the FINDSPACE module of EXPO 2014⁵³ indicated the most
4 probable space group as P2₁/a for **2** and **4**, which were used for structure solution. The unit cell
5 parameters and space group assignments were validated by a Le-Bail fit of PXRD data using a
6 pseudo-Voigt peak profile function⁵⁴ with FOX⁵⁵. For **3**, however, the probable space groups
7 indicated by EXPO 2014 were P2, P2₁, Pm, P2/m, P2₁/m and P2₁/n. Of these, the frequency of
8 occurrence of P2, Pm, P2/m and P2₁/m among the structures in the CSD (version 5.35, 2014
9 release) is very sparse (0.1-0.5%), thus the likely space group of **3** was P2₁/n or P2₁, and
10 structure solution was attempted with both space groups. Structure solution of **2-4** was carried
11 out by global optimization of structural models in direct space based on a Monte-Carlo search
12 using the simulated annealing technique (in parallel tempering mode), as implemented in the
13 program FOX⁵⁵. The optimization of isolated molecules was performed using the energy
14 gradient method as incorporated in MOPAC 9.0⁵⁶. In **3**, the best fit to the experimental data was
15 found for space group P2₁/n.
16
17
18
19
20
21
22
23
24
25

26 The best solution (i.e. the structure with lowest R_{wp}) was used as the initial structural
27 model of **2-4** for Rietveld refinement⁵⁷, which was carried out using the GSAS program⁵⁸. A
28 pseudo-Voigt peak profile function was used during refinement and the background of the
29 PXRD patterns in **2-4** was modeled by a shifted Chebyshev function of the first kind with 20
30 points regularly distributed over the entire 2θ range. Initially, the lattice parameters, background
31 coefficients and profile parameters were refined followed by the refinement of the positional
32 coordinates of all non-hydrogen atoms. Standard restraints were applied to bond lengths and
33 bond angles, and planar restraints were used for phenyl groups in **2-4**. A common isotropic
34 displacement parameter was refined for non-hydrogen atoms. Hydrogen atoms in molecules **2-4**
35 were placed in calculated positions with fixed U_{iso} values. In the final stages of refinement, a
36 preferred orientation correction using the generalized spherical harmonic model was applied. The
37 final Rietveld plots of **2-4** (Fig. 1) showed good agreement between the observed PXRD profile
38 and calculated powder pattern, although the observed powder profile of **3** had few very weak
39 peaks in the 2θ region of 4-11° (intensity < 1% of the maximum peak) presumably due to
40 unknown impurity. The molecular views of **2-4** including the atom labeling scheme are shown
41 in Fig. 2. A summary of crystal data and relevant refinement parameters for **2-4** is listed in Table
42
43
44
45
46
47
48
49
50
51
52
53
54
55
56
57
58
59
60

Hirshfeld Surface Analysis

Hirshfeld Surfaces⁵⁹⁻⁶¹ and associated 2D-fingerprint plots⁶²⁻⁶⁵ were calculated using Crystal Explorer⁶⁶, which accepts a structure input file in the CIF format. For each point on the Hirshfeld isosurface, two distances d_e , the distance from the point to the nearest nucleus external to the surface, and d_i , the distance to the nearest nucleus internal to the surface, are defined. The normalized contact distance (d_{norm}) based on d_e and d_i is given by

$$d_{norm} = \frac{d_i - r_i^{vdW}}{r_i^{vdW}} + \frac{d_e - r_e^{vdW}}{r_e^{vdW}} \quad (1)$$

, where r_i^{vdW} and r_e^{vdW} being the van der Waals radii of the atoms. The value of d_{norm} is negative or positive depending on intermolecular contacts being shorter or longer than the van der Waals separations. The parameter d_{norm} displays a surface with a red-white-blue color scheme, where bright red spots highlight shorter contacts, white areas represent contacts around the van der Waals separation, and blue regions are devoid of close contacts.

Computational Study

Density Functional Theory (DFT) calculations were performed in the solid state (periodic) for **2-4** with the Dmol³ code⁶⁷ in the framework of a generalized gradient approximation (GGA)⁶⁸. The geometry optimization was carried out using BLYP correlation functional^{69,70} with a double numeric plus basis set. The starting atomic coordinates were taken from the final X-ray refinement cycle and geometry optimization was carried out without any structural constraints.

The molecular electrostatic potential (MEP) is an effective tool for identifying and ranking the hydrogen bond donating and accepting sites in organic compounds^{34, 35}. The electrostatic potential at any point \vec{r} in the space surrounding a molecule can be expressed by

$$V(\vec{r}) = \sum_A \frac{z_A}{|\vec{R}_A - \vec{r}|} - \int \frac{\rho(\vec{r}') d\vec{r}'}{|\vec{r} - \vec{r}'|} \quad (2)$$

, where z_A is the charge of the nucleus A located at \vec{R}_A and $\rho(\vec{r})$ is the molecular electron density function. The sign of $V(\vec{r})$ at a particular region depends upon whether the effect of the nucleus or the electrons is dominant there. The MEP surfaces of **2-4** were generated and the electron densities including esp charges were evaluated using an isolated molecule DFT calculation

1
2
3 starting with the geometry optimized models as input in the Dmol³ code with the same set up as
4 earlier. The electrostatic potentials were plotted on 0.017 au electron density isosurface⁷¹. The
5 MEP surfaces have been mapped with a rainbow color scheme with red representing the highest
6 negative potential region while blue representing the highest positive potential region.
7
8
9

10 11 12 **Result and discussion**

13
14
15 The essential difference between nimesulide (**1**) and compounds (**2-4**) is that the nitro
16 group at the C-3 position in **1** has been replaced by different electron donating moieties, a
17 pyrrolidine-2,5-dione in **2** and substituted benzosulfonamide and acetamide derivatives in **3** and
18 **4**, respectively. The overall conformation of molecules in **2-4** can be described by relative
19 orientations of oxo-bridged phenyl rings (A: C1-C6 atoms and B: C8-C13 atoms) as well as the
20 substituents at C-3 position (Fig. 1). The dihedral angles between the least squares planes
21 through rings A and B in **2-4** are 86.46(12), 68.74(13) and 68.77(13)°, respectively; the
22 corresponding angles in two polymorphs of nimesulide, WINWUL(**1a**)⁷² and WINWUL01(**1b**)⁷³
23 are 74.9(2)° and 72.3(2)/76.4(2)°, respectively. While in **2**, the pyrrolidin ring at C-3 position is
24 twisted about the C3-N2 bond with respect to the phenyl ring A by 69.7(2)°, the benzene
25 sulfonamide (N2/S2/O4/O5/C14-C19) fragment in **3** exhibits a syn configuration with respect to
26 ring A; the torsion angle C3-N2-S2-C14 is -51.6(5)°. The conformation of carbamoylbutanoic
27 acid moiety in **4** is established by torsion angles C3-N2-C14-C15 of 176.0(4)°, C14-C15-C16-
28 C17 of -53.6(5)° and C16-C17-C18-O6 of -142.1(7)°. The difference in orientation of the
29 methanesulfonamide group in compounds is revealed by torsion angle C6-N1-S1-C7 of 65.5(5)°
30 in **2**, -53.1(4)° in **3** and 74.9(5)° in **4**; the corresponding values in the nimesulide polymorphs are
31 59.2(3)° in **1a**, -61.1(5)° and -60.2(5)° in **1b**, respectively. An overlay of molecular
32 conformations of the title compounds as determined by X-ray powder diffraction analysis and
33 theoretical calculations (solid state DFT) is shown in Fig. 3. The r.m.s. deviations of the
34 geometrically optimized bond lengths and bond angles from the corresponding
35 crystallographically determined values are 0.02Å, 1.6° in **2**, 0.03Å, 2.2° in **3** and 0.03Å, 2.6° in
36 **4**. Close agreement between the X-ray analyzed structure and that obtained via quantum-
37 mechanical calculations probably indicates that the compounds studied are stable conformers.
38
39
40
41
42
43
44
45
46
47
48
49
50
51
52
53
54

55
56 The crystal packing in **2-4** exhibits an interplay of intermolecular N-H...O, O-H...O, C-
57 H...O and C-H... π (arene) hydrogen bonds (Table 2). A pair of intermolecular N-H...O hydrogen
58
59
60

1
2
3
4
5
6
7
8
9
10
11
12
13
14
15
16
17
18
19
20
21
bonds in **2** (Table 2) with sulfonamide N1 atom in the molecule at (x, y, z) acting as a donor to sulfonyl O2 atom in the molecule at (1-x, 1-y, -z) produces a centrosymmetric dimeric ring (M) with an $R^2_2(8)$ graph-set motif⁷⁴. Similarly, the C7-H7B...O1 hydrogen bonds (Table 2) form another type of $R^2_2(8)$ ring (N). Two types of $R^2_2(8)$ rings are spiro-fused to generate a $C^2_2(8)$ chain along the [001] direction with a MNMN... sequence (Fig. 4). Intermolecular C2-H2...O4 hydrogen bonds in **2** connect parallel $C^2_2(8)$ chains along the [010] direction to form two-dimensional molecular sheets parallel to the (200) plane, which on further linking through C16-H16A...O4 hydrogen bonds results into a three dimensional supramolecular architecture (Fig. 4). Additional reinforcement within the three dimensional framework in **2** is provided by C17-H17B... π (C8-C13) hydrogen bond (Table 2).

22
23
24
25
26
27
28
29
30
31
32
33
34
35
36
37
38
39
40
41
42
43
44
45
46
47
Among the three available NH donors in **3**, N1H and N2H groups participate in intramolecular N-H...O interaction while the remaining N3H group takes part in intermolecular N-H...O hydrogen bonding. Intermolecular N3-HN3...O6 and C7-H7C...O1 hydrogen bonds in **3** (Table 2) connect molecules into two $C^1_1(4)$ chains propagating along the [010] direction, which in turn combine to form a one-dimensional molecular strip built with edge-fused $R^2_2(32)$ synthon of dimension $9.9\text{\AA} \times 5.1\text{\AA}$ (Fig. 5). The parallel strips are further joined through C7-H7B...O6 hydrogen bonds producing $R^3_3(12)$ rings into a two-dimensional framework (Fig 5) parallel to the ($\bar{1}01$) plane. In **4**, while O6-HO6...O4 hydrogen bonds between the centrosymmetrically related molecules facilitate formation of $R^2_2(18)$ rings, N2-HN2...O2 hydrogen bonds generate $C^2_2(18)$ chains propagating along the [100] direction. A combination of $C^2_2(18)$ chains and $R^2_2(18)$ rings produces a columnar architecture. The molecular columns in **4** with axis parallel to the [010] direction are edge-fused along the crystallographic a-axis (Fig. 6). Finally, C10-H10...O5 hydrogen bonds expand the columnar assembly in **4** along the [001] direction into a three dimensional supramolecular framework.

48
49
50
51
52
53
54
55
56
57
58
59
60
The Hirshfeld surfaces of **2-4** are illustrated in Fig. 7 (i), showing surfaces that have been mapped over a d_{norm} range of 0.5 to 1.5 Å. The dominant interaction between the amine NH group and the sulfonyl O atom in **2** and **4** (carbonyl O atom in **3**) can be seen in the Hirshfeld surface (Fig. 7 (i)) as bright red spots labeled as 'a' and 'a'', while almost equally bright red spots (b/b') in Fig. 5(i) are due to the O-H...O hydrogen bond in **4**. The light red areas marked as c/c' in Fig. 7 (i) can be attributed to the C-H...O hydrogen bonds in **2-4**. Other visible red patches (d and e) in Fig. 7 (i) for **2** and **3** correspond to C...O and H...H interactions,

1
2
3
4
5
6
7
8
9
10
11
12
13
14
15
16
17
18
19
20
21
22
23
24
25
26
27
28
29
30
31
32
33
34
35
36
37
38
39
40
41
42
43
44
45
46
47
48
49
50
51
52
53
54
55
56
57
58
59
60

respectively. In the 2D fingerprint plots (Fig. 7 (ii)), two sharp spikes (labeled as 'a' and 'a') of almost equal length in the region $2.1 < d_e + d_i < 2.5$ Å are characteristics of N-H...O interactions. The spikes (labeled as b/b' and c/c') due to O-H...O and C-H...O hydrogen bonds in **2-4** are masked within the corresponding N-H...O spikes (a/a') in Fig. 7 (ii). The wings marked with black circles in Fig. 7 (ii) represent the C-H... π interaction in **2**. The central spikes (Fig. 7 (ii)) extending upto (d_i , d_e) region of (1.1Å, 1.1Å) in **2**, (0.9Å, 0.9Å) in **3** and (0.95Å, 0.95Å) in **4** reveal relatively high percentages of H...H contacts in **2-4**. The sharpness of central spike in Fig. 7 (ii) is a consequence of close H...H contacts (~ 2.02 Å) in **3**. The subtle differences among the molecular interactions in **2-4** are reflected in the distribution of scattered points in both high and low (d_i , d_e) regions in the fingerprint plots (Fig. 7 (ii)). The relative contribution of different interactions to the Hirshfeld surfaces of **2-4** as well as the two nimesulide polymorphs (**1a**, **1b**) and a few nimesulide derivatives with different substitutions at the C3 position (Fig. 2) retrieved from the CSD is shown in Fig. 8. It is evident from Fig. 8 that H...H, O...H and C...H interactions in **2-4** can account for more than 90% of the Hirshfeld surface area (92.1% in **2**, 91.9% in **3** and 93.5% in **4**), whereas the corresponding values are 84.2% in **1a**, 84.4% in **1b**, and 86.2% in 2,5-dioxodihydropyrrol-1-yl derivative (MUTJUH)⁷⁵ of nimesulide, which has a close structural resemblance with **2**. Due to replacement of the nitro group in nimesulide by different cyclic and acyclic substituents in **2-4**, the contribution of H...H interactions increased steadily from 31.7% in **1b** to 42.3% in **2** with a corresponding decrease in the contribution of C...O contacts from 6.9% in **1a** to 1.0% in **4**. A possible explanation for enhanced H...H interaction contribution to the Hirshfeld surface area in **2-4** is the increased percentage of hydrogen atoms in the molecular formula (39-43%) in comparison to that of nimesulide (36%).

The effect of substitutions in the nimesulide skeleton on the formation of supramolecular synthon has been summarized in Table 3. In nimesulide polymorphs (**1a** and **1b**) with a strong electron withdrawing nitro (NO₂) group at the trans position with respect to the methanesulfonamide moiety, the N(sulfonamide)-H...O(sulfonyl) hydrogen bond generates one-dimensional molecular tapes comprising of C₂²(16) synthon. When the nitro group in **1** is replaced by a strong electron donating amino (NH₂) group in OPEKOK⁵⁰, the N atom acts as a double donor to two sulfonyl O atoms to produce two C₂²(18) chains which combine together into a two-dimensional supramolecular assembly built with fused R₂²(12) and R₂²(36) rings. The replacement of NO₂ group in **1** by bulky cyclic substituents, such as dioxopyrrolidin-1-yl in **2**,

dioxopyrrol-1-yl in MUTJUH⁷⁵, dioxoisindole-2-yl in OPEKUQ⁵⁰, phenyl-1H-triazol-1-yl in QOJSAL⁷⁶, tolyl-1H-triazol-1-yl in QOJSEP⁷⁶ and chloromethyl phenoxyethyl-1H-triazol-1-yl in QOJSIT⁷⁶ leads to different hydrogen bonding patterns. The molecular assembly in these compounds exhibits cyclic $R_2^2(8)$ ring generated by N(sulfonamide) -H...O(sulfonyl) hydrogen bonds. The propagation of $R_2^2(8)$ rings via C(aryl)-H...O(sulfonyl) and C(aryl)-H...O(oxopyrrol) hydrogen bonds results in different supramolecular framework in these structures. In **3** and **4**, with acyclic substituents having multiple NH donors replacing the NO₂ group in **1**, the molecular aggregation, however, reveals $C_m^n(x)$ chains formed by N(amide)-H...O(amide) and N(amide)-H...O(sulfonyl) hydrogen bonds. The ranking of different donor and acceptor groups in intermolecular hydrogen bonding in **2-4** and other NO₂ substituted nimesulide derivatives has been further confirmed by MEP calculations.

The MEP surfaces of **2-4** (Fig. 9) as well as the nimesulide polymorphs (**1a** and **1b**) and a few NO₂ substituted nimesulide derivatives containing different hydrogen bond donors such as -NH, -OH and -CH groups have been analyzed successfully in relation to their hydrogen bonding. The MEP derived charges at the BLYP level using DMol³ for atoms in **2-4** indicated high negative charges on the oxygen (O1-O5 in **2**, O1-O6 in **3** and **4**) as well as the nitrogen (excepting the pyrrolidin ring N2 in **2**) atoms. The sulfur (S1 in **2**, **4** and S1, S2 in **3**) and carbon (C5, C8, C14, C15 in **2**, C3, C5, C8, C20 in **3**, C3, C5, C8, C14, C18 in **4**) atoms carry substantial positive charge due to electron withdrawing nature of adjacent oxygen and nitrogen atoms. Significant positive charge accumulation on the hydrogen atoms (HN1 in **2**; HN1, HN2, HN3 in **3**; HN1, HN2, HO6 in **4**) of amino and hydroxyl moieties in **2-4** suggests that these groups are likely to act as donors in intra- and inter-molecular D-H...X hydrogen bonds. Due to this charge re-distribution the dipole moments of **2-4** become 2.64, 3.75 and 4.26 a.u., respectively. The magnitudes of electrostatic potential maxima ($V_{s,max}$) associated with the hydrogen atoms of **1-4** can serve as indicators of a fairly realistic ranking of hydrogen bond donating ability, and the corresponding $V_{s,min}$ values can be used to identify and rank hydrogen bond acceptor sites. The magnitudes of $V_{s,max}$ and $V_{s,min}$ values associated with the donor/acceptor groups of **1-4** and other related compounds are related to the relative strength of N-H...O, O-H...O and C-H...O hydrogen bonds (Table 4). In the nimesulide polymorphs (**1a** and **1b**), the hydrogen atoms of sulfonamide NH and oxygen atoms of the nitro group are associated with the maximum (51-56 Kcal mol⁻¹) and minimum (-37 to -39 Kcal mol⁻¹) MEP values (Table

1
2
3
4 4). This is consistent with the crystallographic observation which indicates that N(sulfonamide)-
5 H...O(nitro) is the strongest intermolecular hydrogen bond in nimesulide^{72,73}. Three most positive
6 potentials in **2** correspond to hydrogen atoms of the amino group, HN1 ($V_{s,max}$ 51 Kcal mol⁻¹),
7 and pyrrolidin ring, H16 and H17 ($V_{s,max}$ 36-37 Kcal mol⁻¹), which participate in hydrogen
8 bonding (Table 2). The hydrogen bond acceptors in **2**, on the other hand are characterized by
9 three strong negative potentials around the oxygen atoms of sulfonyl and oxo groups with O1
10 and O2 ($V_{s,min}$ -39 Kcal mol⁻¹) and O4 and O5 ($V_{s,min}$ -35 Kcal mol⁻¹), respectively. The
11 electrostatic potentials near the bridging oxygen atom O3 in **2-4** lie in the range -2 to -10 Kcal
12 mol⁻¹. The presence of different electron withdrawing substituents can significantly modify the
13 molecular electrostatic potential around phenyl rings³⁷. While regions of negative electrostatic
14 potentials of -9 Kcal mol⁻¹ above and below the terminal benzene ring (C8-C13 atoms) in **2**
15 reflect the π electrons taking part in C-H... π hydrogen bond, no such local minima could be
16 observed for other aryl rings in **2-4**.
17
18
19
20
21
22
23
24
25

26 In **3**, the amino hydrogen (HN3) is localized in the most positive potential region, $V_{s,max}$
27 of 75 Kcal mol⁻¹, while the carbonyl oxygen atom (O6) assumes the top ranked negative surface
28 potential of $V_{s,min}$ -40 Kcal mol⁻¹. This indicates that among different NH donors and oxygen
29 acceptors, the acetamide N/O part (N3 and O6 atoms) is favored for a relatively strong N-H...O
30 hydrogen bond. The $V_{s,max}$ values associated with HN1 and HN2 atoms participating in
31 intramolecular N-H...O interaction in **3**, are 53 and 62 Kcal mol⁻¹, respectively. The N2-
32 HN2...O2 and O6-HO6...O4 intermolecular hydrogen bonds in **4** are characterized by two top
33 ranked positive molecular electrostatic potentials associated with HO6 ($V_{s,max}$ 79 Kcal mol⁻¹) and
34 HN2 ($V_{s,max}$ 65 Kcal mol⁻¹) atoms and corresponding most negative potentials around O2 and
35 O4 ($V_{s,min}$ -46 Kcal mol⁻¹) atoms. Other strong negative potential near O5 ($V_{s,min}$ -45 Kcal mol⁻¹)
36 and a moderate positive potential of 32 Kcal mol⁻¹ around H10 can be attributed to C10-
37 H10...O5 intermolecular hydrogen bond in **4**. Similar correlation between the MEP values of
38 donor/acceptor atoms and intermolecular hydrogen bond interaction can also be established for
39 other NO₂ substituted nimesulide derivatives (Table 4), where most positive and most negative
40 potential values correspond to strongest hydrogen bonds.
41
42
43
44
45
46
47
48
49
50
51
52
53
54
55
56
57
58
59
60

Conclusions

In summary, crystal structures of three nimesulide derivatives (**2-4**), in which pyrrolidin-2,5-dione (in **2**), substituted benzosulfonamide (in **3**) and acetamide (in **4**) moieties replacing the nitro group at the C-3 position in nimesulide (**1**), have been determined using powder crystal X-ray diffraction (PXRD). The subtleties of crystal packing are illustrated by an interplay of N-H...O, O-H...O, C-H...O and C-H... π (in **2**) hydrogen bonds, which assemble molecules in compounds **2-4** into supramolecular architecture via the formation of $R_m^n(x)$ rings and $C_m^n(x)$ polymeric chains. The results also emphasize that a reliable ranking of hydrogen bond donor strength in **2-4** can be achieved by using molecular electrostatic potential (MEP) surfaces and for competing hydrogen bond donors, the selection depends strongly on the MEP values of the acceptor. The MEP based selectivity of hydrogen bonding can be used for designing tailor-made nimesulide derivatives with desired biological activity. A comparison of the relative contribution of different interactions to the Hirshfeld surfaces of **2-4** and a few related nimesulide derivatives indicated that H...H, O...H and C...H interactions can account for more than 80% of the Hirshfeld surface area. Finally, the present work clearly demonstrates the potential of PXRD for determining the crystal structure of complex organic materials with considerable molecular flexibility directly from the bulk powder without the need to grow single crystals.

Acknowledgements:

Financial support from the Council for Scientific and Industrial Research (CSIR), New Delhi, India, for a senior research fellowship (SRF) to T.D, is gratefully acknowledged.

Supporting Information: Crystallographic data for the structures $C_{17}H_{16}O_5N_2S$ (**2**), $C_{21}H_{21}O_6N_3S_2$ (**3**) and $C_{18}H_{20}O_6N_2S$ (**4**) reported in this article have been deposited to the Cambridge Crystallographic Data Centre with publication numbers CCDC 1430581-1430583. Copies of the data can be obtained free of charge on application to CCDC, 12 Union Road, Cambridge CB2 1EZ, UK (fax: +44 1223 336033; email: (deposit@ccdc.cam.ac.uk)). Values of selected bond distances, bond angles and torsion angles are given in Table S1. This material is available free of charge via the Internet at <http://pubs.acs.org>.

References

- (1) Steiner, T., *Angew. Chem., Int. Ed.* **2002**, *41*, 48-76.
- (2) Glowacki, E. D.; Irimia-Vladu, M.; Bauer, S.; Sariciftci, N. S., *J. Mater. Chem. B* **2013**, *1*, 3742-3753.
- (3) Sweetman, A. M.; Jarvis, S. P.; Sang, H.; Lekkas, I.; Rahe, P.; Wang, Y.; Wang, J.; Champness, N. R.; Kantorovich, L.; Moriarty, P., *Nat. Commun.* **2014**, *5*.
- (4) Parkinson, G.; Gunasekera, A.; Vojtechovsky, J.; Zhang, X.; Kunkel, T. A.; Berman, H.; Ebright, R. H., *Nat. Struct. Mol. Biol.* **1996**, *3*, 837-841.
- (5) Kool, E. T., *Annu. Rev. Biophys. Biomol. Struct.* **2001**, *30*, 1-22.
- (6) Cleland, W.; Kreevoy, M., *Science* **1994**, *264*, 1887-1890.
- (7) Cleland, W. W.; Frey, P. A.; Gerlt, J. A., *J. Biol. Chem.* **1998**, *273*, 25529-25532.
- (8) Gerlt, J. A.; Kreevoy, M. M.; Cleland, W. W.; Frey, P. A., *Chem. Biol.* **1997**, *4*, 259-267.
- (9) Pauling, L.; Corey, R. B.; Branson, H. R., *Proc. Natl. Acad. Sci. U. S. A.* **1951**, *37*, 205-11.
- (10) Cordier, F.; Grzesiek, S., *J. Am. Chem. Soc.* **1999**, *121*, 1601-1602.
- (11) Hoof, R. W. W.; Sander, C.; Vriend, G., *Proteins Struct., Funct., Bioinf.* **1996**, *26*, 363-376.
- (12) Desiraju, G. R., *Acc. Chem. Res.* **2002**, *35*, 565-573.
- (13) *Frontiers in Crystal Engineering*; Tiekink, E. R. T., Vittal, J., Eds.; John Wiley & sons: 2006.
- (14) Brittain, H. G., *J. Pharm. Sci.* **2012**, *101*, 464-484.
- (15) Serajuddin, A. T. M., *Adv. Drug Delivery Rev.* **2007**, *59*, 603-616.
- (16) Vishweshwar, P.; McMahon, J. A.; Bis, J. A.; Zaworotko, M. J., *J. Pharm. Sci.* **2006**, *95*, 499-516.
- (17) Schultheiss, N.; Newman, A., *Cryst. Growth Des.* **2009**, *9*, 2950-2967.
- (18) Desiraju, G. R., *Nature* **2001**, *412*, 397-400.
- (19) Allen, F. H.; Motherwell, W. D. S.; Raithby, P. R.; Shields, G. P.; Taylor, R., *New J. Chem.* **1999**, *23*, 25-34.

- 1
2
3
4 (20) Desiraju, G. R.; Steiner, T., *The Weak Hydrogen Bond in Structural Chemistry and*
5 *Biology*.; Oxford University Press: 2001.
6
7 (21) Moulton, B.; Zaworotko, M. J., *Chem. Rev.* **2001**, *101*, 1629-1658.
8
9 (22) Jeffrey, G. A., *An Introduction to Hydrogen Bonding*.; Oxford University Press: New
10 York, 1997.
11
12 (23) Braga, D.; Grepioni, F.; Biradha, K.; Pedireddi, V. R.; Desiraju, G. R., *J. Am. Chem. Soc.*
13 **1995**, *117*, 3156-3166.
14
15 (24) Spek, A. L., *Acta Crystallogr. D* **2009**, *65*, 148-155.
16
17 (25) Etter, M. C., *Acc. Chem. Res.* **1990**, *23*, 120-126.
18
19 (26) Etter, M. C., *J. Phys. Chem.* **1991**, *95*, 4601-4610.
20
21 (27) Aakeröy, C. B.; Baldrighi, M.; Desper, J.; Metrangolo, P.; Resnati, G., *Chem. - Eur. J.*
22 **2013**, *19*, 16240-16247.
23
24 (28) Duggirala, N. K.; Wood, G. P. F.; Fischer, A.; Wojtas, L.; Perry, M. L.; Zaworotko, M.
25 J., *Cryst. Growth Des.* **2015**, *15*, 4341-4354.
26
27 (29) Dey, A.; Bera, S.; Biradha, K., *Cryst. Growth Des.* **2015**, *15*, 318-325.
28
29 (30) Lü, J.; Han, L.-W.; Alsmail, N. H.; Blake, A. J.; Lewis, W.; Cao, R.; Schröder, M., *Cryst.*
30 *Growth Des.* **2015**, *15*, 4219-4224.
31
32 (31) Hunter, C. A., *Angew. Chem., Int. Ed.* **2004**, *43*, 5310-5324.
33
34 (32) Musumeci, D.; Hunter, C. A.; Prohens, R.; Scuderi, S.; McCabe, J. F., *Chem. Sci.* **2011**, *2*,
35 883-890.
36
37 (33) Murray, J. S.; Politzer, P., *J. Org. Chem.* **1991**, *56*, 6715-6717.
38
39 (34) Politzer, P.; Murray, J. S., *Cryst. Growth Des.* **2015**, *15*, 3767-3774.
40
41 (35) Aakeroy, C. B.; Wijethunga, T. K.; Desper, J., *New J. Chem.* **2015**, *39*, 822-828.
42
43 (36) Aakeröy, C. B.; Epa, K.; Forbes, S.; Schultheiss, N.; Desper, J., *Chem.- Eur. J.* **2013**, *19*,
44 14998-15003.
45
46 (37) Bulat, F. A.; Toro-Labbe, A.; Brinck, T.; Murray, J. S.; Politzer, P., *J. Mol. Model* **2010**,
47 *16*, 1679-91.
48
49 (38) Harris, K. D. M.; Tremayne, M.; Kariuki, B. M., *Angew. Chem., Int. Ed.* **2001**, *40*, 1626-
50 1651.
51
52 (39) David, W. I. F.; Shankland, K., *Acta Crystallogr. A* **2008**, *64*, 52-64.
53
54 (40) *Structure Determination from Powder Diffraction Data*.; David, W. I. F., Shankland, L.,
55 McCusker, L. B., Baerlocher, Ch., Eds.; Oxford University Press: New York, 2002.
56
57
58
59
60

- 1
2
3 (41) Pagola, S.; Stephens, P. W.; Bohle, D. S.; Kosar, A. D.; Madsen, S. K., *Nature* **2000**, *404*,
4 307-310.
5
6 (42) Harris, K. D. M.; Cheung, E. Y., *Chem Soc. Rev.* **2004**, *33*, 526-538.
7
8 (43) Hammond, R. B.; Roberts, K. J.; Docherty, R.; Edmondson, M., *J. Phys. Chem. B* **1997**,
9 *101*, 6532-6536.
10
11 (44) Favre-Nicolin, V.; Černý, R., *Z. Kristallogr. Cryst. Mat.* **2004**, *219*, 847-856.
12
13 (45) Brodski, V.; Peschar, R.; Schenk, H., *J. Appl. Crystallogr.* **2005**, *38*, 688-693.
14
15 (46) Griswold, D. E.; Adams, J. L., *Med. Res. Rev.* **1996**, *16*, 181-206.
16
17 (47) Traversa, G.; Bianchi, C.; Da Cas, R.; Abraha, I.; Menniti-Ippolito, F.; Venegoni, M., *Br.*
18 *Med. J.* **2003**, *327*, 18-22.
19
20 (48) Hawkey, C. J., *Gastroenterology* **2000**, *119*, 521-35.
21
22 (49) Durgadas, S.; Chatare, V. k.; Mukkanti, K.; Pal, S., *Appl. Org. Chem.* **2010**, *24*, 680-684.
23
24 (50) Bhattacharya, A.; Ghosh, S.; Kankanala, K.; Reddy, V. R.; Mukkanti, K.; Pal, S.;
25 Mukherjee, A. K., *Chem. Phys. Lett.* **2010**, *493*, 151-157.
26
27 (51) Karakuş, S.; Güniz Küçükgülzel, Ş.; Küçükgülzel, İ.; De Clercq, E.; Pannecouque, C.;
28 Andrei, G.; Snoeck, R.; Şahin, F.; Faruk Bayrak, Ö., *Eur. J. Med. Chem.* **2009**, *44*, 3591-3595.
29
30 (52) Altomare, A.; Giacobazzo, C.; Guagliardi, A.; Moliterni, A. G. G.; Rizzi, R.; Werner, P.-
31 E., *J. Appl. Crystallogr.* **2000**, *33*, 1180-1186.
32
33 (53) Altomare, A.; Cuocci, C.; Giacobazzo, C.; Moliterni, A.; Rizzi, R.; Corriero, N.;
34 Falcicchio, A., *J. Appl. Crystallogr.* **2013**, *46*, 1231-1235.
35
36 (54) Thompson, P.; Cox, D. E.; Hastings, J. B., *J. Appl. Crystallogr.* **1987**, *20*, 79-83.
37
38 (55) Favre-Nicolin, V.; Cerny, R., *J. Appl. Crystallogr.* **2002**, *35*, 734-743.
39
40 (56) Stewart, J. J., *J. Mol. Model.* **2007**, *13*, 1173-213.
41
42 (57) Rietveld, H., *Acta Crystallogr.* **1967**, *22*, 151-152.
43
44 (58) Larson, A. C.; Von Dreele, R. B. *General Structure Analysis System (GSAS)*; Los Alamos
45 Laboratory Report, LAUR: 2000; pp 86-748.
46
47 (59) Hirshfeld, F. L., *Theor. Chim. Acta* **1977**, *44*, 129-138.
48
49 (60) Spackman, M. A.; Jayatilaka, D., *CrystEngComm* **2009**, *11*, 19-32.
50
51 (61) Clausen, H. F.; Chevallier, M. S.; Spackman, M. A.; Iversen, B. B., *New J. Chem.* **2010**,
52 *34*, 193-199.
53
54 (62) Spackman, M. A.; McKinnon, J. J., *CrystEngComm* **2002**, *4*, 378-392.
55
56
57
58
59
60

- 1
2
3
4
5
6
7
8
9
10
11
12
13
14
15
16
17
18
19
20
21
22
23
24
25
26
27
28
29
30
31
32
33
34
35
36
37
38
39
40
41
42
43
44
45
46
47
48
49
50
51
52
53
54
55
56
57
58
59
60
- (63) Parkin, A.; Barr, G.; Dong, W.; Gilmore, C. J.; Jayatilaka, D.; McKinnon, J. J.; Spackman, M. A.; Wilson, C. C., *CrystEngComm* **2007**, *9*, 648-652.
- (64) Rohl, A. L.; Moret, M.; Kaminsky, W.; Claborn, K.; McKinnon, J. J.; Kahr, B., *Cryst. Growth Des.* **2008**, *8*, 4517-4525.
- (65) McKinnon, J. J.; Spackman, M. A.; Mitchell, A. S., *Acta Crystallogr. B* **2004**, *60*, 627-668.
- (66) Wolff, S.; Grimwood, D.; McKinnon, J.; Jayatilaka, D.; Spackman, M., *Crystal Explorer 2.1*, University of Western Australia, Perth **2007**.
- (67) Delley, B., *J. Chem. Phys.* **1990**, *92*, 508-517.
- (68) Perdew, J.P.; Burke, K.; Ernzerhof, M., *Phys. Rev. Lett.* **1996**, *77*, 3865-3868.
- (69) Becke, A. D., *Phys. Rev. A* **1988**, *38*, 3098-3100.
- (70) Lee, C.; Yang, W.; Parr, R. G., *Phys. Rev. B* **1988**, *37*, 785-789.
- (71) Bader, R. F. W.; Carroll, M. T.; Cheeseman, J. R.; Chang, C., *J. Am. Chem. Soc.* **1987**, *109*, 7968-7979.
- (72) Dupont, L.; Pirotte, B.; Masereel, B.; Delarge, J.; Geczy, J., *Acta Crystallogr. C* **1995**, *51*, 507-509.
- (73) Sanphui, P.; Sarma, B.; Nangia, A., *J. Pharm. Sci.* **2011**, *100*, 2287-2299.
- (74) Bernstein, J.; Davis, R. E.; Shimoni, L.; Chang, N.-L., *Angew. Chem., Int. Ed.* **1995**, *34*, 1555-1573.
- (75) Bhattacharya, A.; Kankanala, K.; Pal, S.; Mukherjee, A. K., *J. Mol. Struct.* **2010**, *975*, 40-46.
- (76) Dey, T.; Ghosh, S.; Mareddy, J.; Anireddy, J.; Pal, S.; Mukherjee, A. K., *CrystEngComm* **2015**, *17*, 764-774.

Tables

Table 1 Crystal data and structure refinement parameters of C₁₇H₁₆O₅N₂S (**2**), C₂₁H₂₁O₆N₃S₂ (**3**) and C₁₈H₂₀O₆N₂S (**4**).

| Compound | C ₁₇ H ₁₆ O ₅ N ₂ S (2) | C ₂₁ H ₂₁ O ₆ N ₃ S ₂ (3) | C ₁₈ H ₂₀ O ₆ N ₂ S (4) |
|---|--|---|--|
| Formula weight | 360.39 | 475.55 | 392.43 |
| Temperature (K) | 293(2) | 293(2) | 293 (2) |
| Crystal system | Monoclinic | Monoclinic | Monoclinic |
| Wavelength (Å) | 1.5418 | 1.5406 | 1.5418 |
| Space group | P2 ₁ /a | P2 ₁ /n | P2 ₁ /a |
| a (Å) | 32.7832(5) | 23.5927(7) | 18.791(4) |
| b (Å) | 5.8150(2) | 5.1184(2) | 8.967(2) |
| c (Å) | 8.8234(1) | 17.7026(5) | 11.339(3) |
| α (°) | 90 | 90 | 90.000 |
| β (°) | 90.450(2) | 93.745(3) | 104.525(2) |
| γ (°) | 90 | 90 | 90.000 |
| Volume (Å ³) | 1682.0(1) | 2133.1(1) | 1849.5(8) |
| Z | 4 | 4 | 4 |
| Density (calculated) g cm ⁻³ | 1.4232 | 1.4808 | 1.4094 |
| 2θ interval (°) | 4-96 | 4-90 | 6-100 |
| Step size (°) | 0.02 | 0.02 | 0.02 |
| Counting time (sec) | 20 | 20 | 20 |
| No. of variable parameters | 209 | 191 | 219 |
| No. of background points | 20 | 20 | 25 |
| Spherical harmonics | 18 | 14 | 18 |
| R _p | 0.0412 | 0.0198 | 0.0255 |
| R _{wp} | 0.0585 | 0.0276 | 0.0349 |
| R _F ² | 0.0569 | 0.1096 | 0.0936 |
| χ ² /S | 2.334 | 2.119 | 2.374 |

Table 2 Hydrogen bonds in C₁₇H₁₆O₅N₂S (**2**), C₂₁H₂₁O₆N₃S₂ (**3**) and C₁₈H₂₀O₆N₂S (**4**).

| Interaction | D-H/ Å | H...A/ Å | D...A/ Å | D-H...A/ ° | Symmetry code |
|--|--------|----------|-----------|------------|---------------------|
| C₁₇H₁₆O₅N₂S (2) | | | | | |
| N1-HN1...O2 | 0.86 | 2.20 | 2.913(6) | 139 | 1-x, 1-y, -z |
| C2-H2...O4 | 0.93 | 2.55 | 3.449(11) | 164 | x, 1+y, z |
| C7-H7B...O1 | 0.96 | 2.53 | 3.407(6) | 152 | 1-x, 1-y, 1-z |
| C16-H16A...O4 | 0.97 | 2.52 | 3.203(13) | 128 | 1/2-x, 1/2+y, 1-z |
| C17-H17B...Cg(2) | 0.96 | 2.77 | | 140 | 1/2-x, 1/2+y, -z |
| C₂₁H₂₁O₆N₃S₂ (3) | | | | | |
| N1-HN1...O2 | 0.87 | 2.47 | 2.459(7) | 79 | x, y, z |
| N2-HN2...O4 | 0.86 | 2.49 | 2.460(6) | 78 | x, y, z |
| N3-HN3...O6 | 0.86 | 2.19 | 3.041(6) | 169 | x, -1+y, z |
| C7-H7B...O6 | 0.95 | 2.54 | 3.419(13) | 154 | 1/2+x, 5/2-y, 1/2+z |
| C7-H7C...O1 | 0.96 | 2.53 | 3.344(6) | 142 | x, -1+y, z |
| C₁₈H₂₀O₆N₂S (4) | | | | | |
| N2-HN2...O2 | 0.86 | 1.98 | 2.806(9) | 159 | -1/2+x, 1/2-y, z |
| O6-HO6...O4 | 0.83 | 2.00 | 2.804(12) | 163 | -x, 1-y, -z |
| C10-H10...O5 | 0.93 | 2.33 | 3.204(10) | 156 | -x, -y, 1-z |
| C17-H17A...O6 | 0.96 | 2.54 | 3.494(6) | 176 | -x, 1-y, -z |
| N1-HN1...N2 | 0.86 | 2.64 | 3.452(5) | 157 | 1/2-x, -1/2+y, 1-z |
| Cg(2) = C8-C13 atoms for 2 | | | | | |

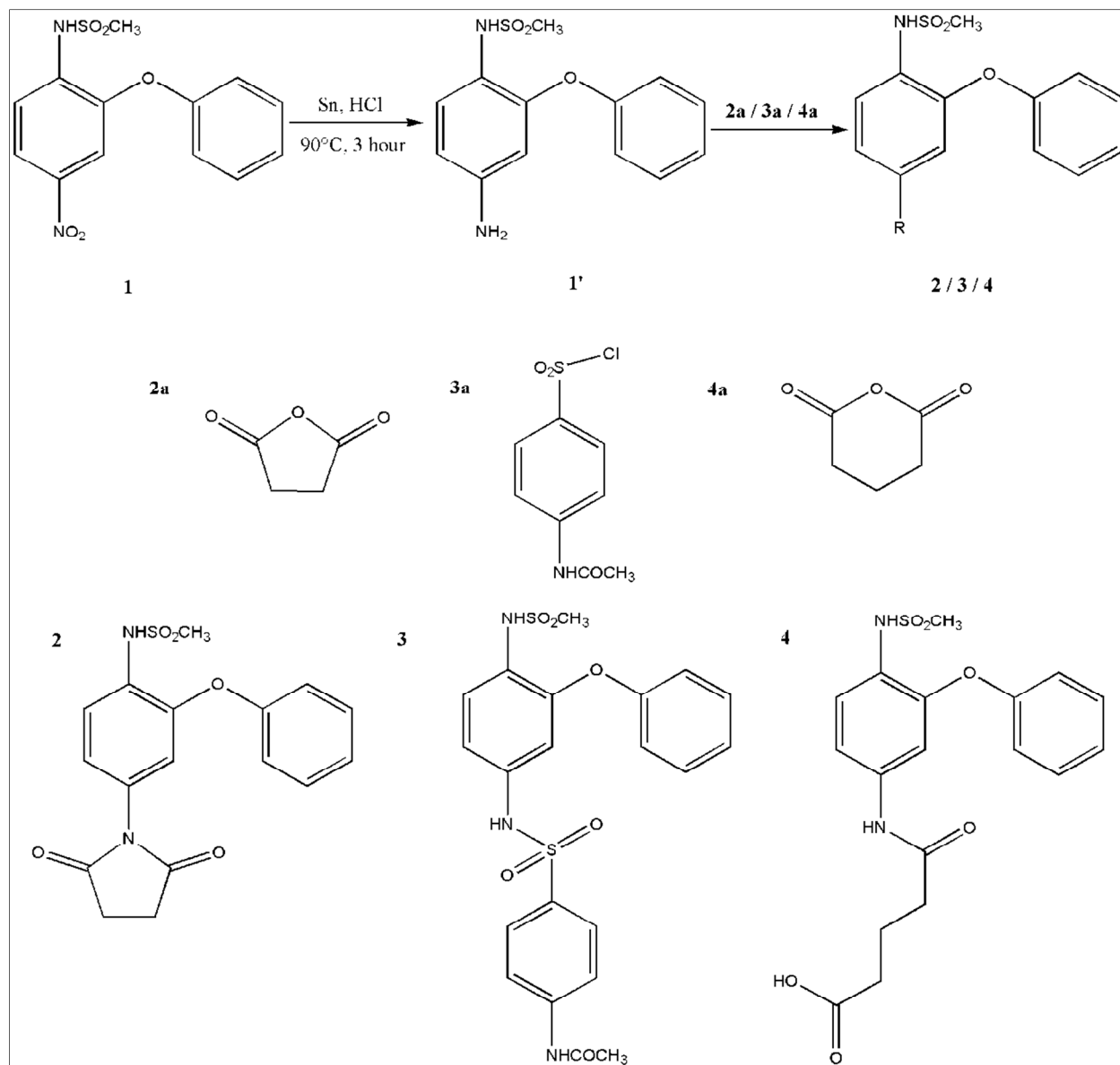
Table 3 Supramolecular assemblies formed by hydrogen bonds in nimesulide and its derivatives

| Compounds | Type of hydrogen bond | D...A (Å) | ∠DHA (°) | Graph Set Notation |
|----------------------|---------------------------------|-------------------|----------|----------------------------------|
| WINWUL (1a) | N(sulfonamide)-H...O(nitro) | 3.092(3) | 151 | C ₂ ² (16) |
| | C(aryl)-H...O(sulfonyl) | 3.459(4) | 154 | C ₂ ² (14) |
| WINWUL01 (1b) | N(sulfonamide)-H...O(nitro) | 3.000(6)/3.079(6) | 151/138 | C ₂ ² (16) |
| | C(aryl)-H...O(sulfonyl) | 3.420(6)/3.463(6) | 160/156 | C ₂ ² (14) |
| MUTJUH | N(sulfonamide)-H...O(sulfonyl) | 3.166(2) | 157 | R ₂ ² (8) |
| | C(methyl)-H...O(sulfonyl) | 3.428(2) | 145 | R ₂ ² (8) |
| OPEKOK | N(amine)-H...O(sulfonyl) | 3.274(4) | 162 | C ₂ ² (18) |
| | N(amine)-H...O(sulfonyl) | 3.179(4) | 147 | C ₂ ² (18) |
| OPEKUQ | N(sulfonamide)-H...O(sulfonyl) | 3.060(2) | 147 | R ₂ ² (8) |
| | C(aryl)-H...O(di-Oxo-Pyrrol) | 3.441(2) | 145 | R ₂ ² (10) |
| | C(methyl)-H...O(sulfonyl) | 3.510(2) | 152 | R ₂ ² (8) |
| QOJSAL | N(sulfonamide)-H...O(sulfonyl) | 2.997(3) | 147 | R ₂ ² (8) |
| | C(methyl)-H...O(sulfonyl) | 3.516(3) | 167 | C ₂ ² (8) |
| | C(triazole)-H...N(triazole) | 3.585(4) | 163 | C ₂ ² (8) |
| QOJSEP | N(sulfonamide)-H...O(sulfonyl) | 2.985(9) | 144 | R ₂ ² (8) |
| | C(aryl)-H...O(oxo-Bridge) | 3.330(3) | 161 | C ₂ ² (12) |
| QOJSIT | N(sulfonamide)-H...O(sulfonyl) | 3.174(7) | 157 | R ₂ ² (8) |
| | C(methyl)-H...O(sulfonyl) | 2.978(9) | 156 | C ₂ ² (8) |
| Compound 2 | N(sulfonamide)-H...O(sulfonyl) | 2.913(6) | 139 | R ₂ ² (8) |
| | C(methyl)-H...O(sulfonyl) | 3.407(6) | 152 | R ₂ ² (8) |
| Compound 3 | N(amide)-H...O(amide) | 3.041(6) | 169 | C ₁ ¹ (4) |
| | C(methyl)-H...O(amide) | 3.344(6) | 142 | C ₁ ¹ (4) |
| Compound 4 | N(amide)-H...O(sulfonyl) | 2.804(9) | 159 | C ₂ ² (18) |
| | O(carboxylic acid)-H...O(amide) | 2.800(12) | 163 | R ₂ ² (18) |

Table 4 Selected $V_{s,max}$ and $V_{s,min}$ values for MEP surfaces of **1-4** and few other nimesulide derivatives.

| Compound | Selected area | $V_{s,max}/V_{s,min}$ (Kcal/mol) |
|--|---|-------------------------------------|
| C₁₇H₁₆O₅N₂S (2) | Sulfonyl oxygens (O1, O2) | -39 |
| | Pyrrolidin oxo group (O4, O5) | -35 |
| | Pyrrolidin hydrogens (H16A, H16B, H17A, H17B) | 36 |
| | Sulfonamide hydrogen (HN1) | 51 |
| C₂₁H₂₁O₆N₃S₂ (3) | Carbonyl oxygen (O6) | -40 |
| | Sulfonyl oxygens (O4, O5) | -38 |
| | Sulfonyl oxygens (O1, O2) | -36 |
| | Sulfonamide hydrogen (HN1) | 53 |
| | Sulfonamide hydrogen (HN2) | 62 |
| | Amide hydrogen (HN3) | 75 |
| C₁₈H₂₀O₆N₂S (4) | Sulfonyl oxygen (O2), Carbonyl oxygen (O4) | -46 |
| | Carbonyl oxygen of COOH (O5) | -45 |
| | Sulfonyl oxygen (O1) | -44 |
| | Sulfonamide hydrogen (HN1) | 46 |
| | Amide hydrogen (HN2) | 65 |
| | Carboxylic acid hydrogen (HO6) | 79 |
| WINWUL (1a) | Nitro oxygen (O3, O4) | -37 |
| | Sulfonamide hydrogen (HN1) | 56 |
| WINWUL01 (1b) | Nitro oxygen (O3, O4) | -39 |
| | Sulfonamide hydrogen (HN1, HN3) | 52 |
| MUTJUH | Sulfonyl oxygen (O2, O3) | -45 |
| | Sulfonamide hydrogen (HN2) | 56 |
| OPEKOK | Sulfonyl oxygen (O2, O3) | -48 |
| | Amino hydrogen (HN1) | 58 |
| OPEKUQ | Sulfonyl oxygen (O3) | -43 |
| | Sulfonamide hydrogen (HN2) | 52 |
| QOJSAL | Sulfonyl oxygen (O2) | -33 |
| | Sulfonamide hydrogen (HN1) | 55 |
| QOJSEP | Sulfonyl oxygen (O2, O3) | -34 |
| | Sulfonamide hydrogen (HN1) | 51 |
| QOJSIT | Sulfonyl oxygen (O2) | -34 |
| | Sulfonamide hydrogen (HN1) | 56 |

Scheme and figures



Scheme 1

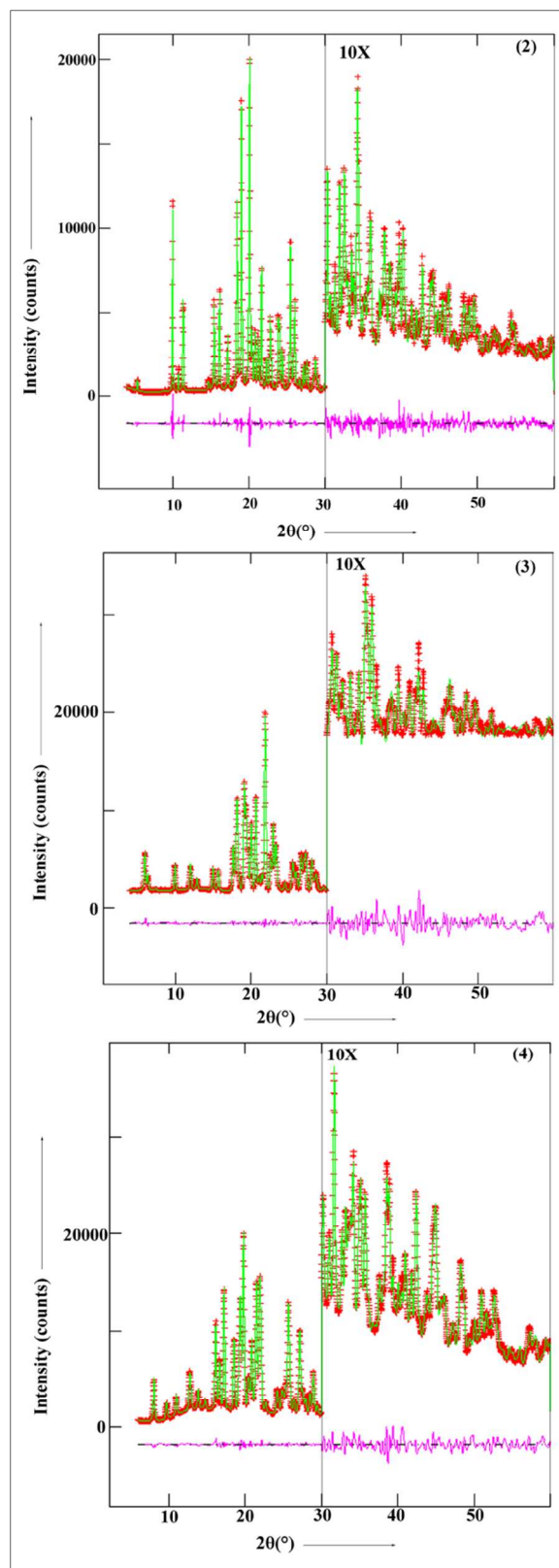


Fig. 1: Final rietveld plot for $C_{17}H_{16}O_5N_2S$ (2), $C_{21}H_{21}O_6N_3S_2$ (3) and $C_{18}H_{20}O_6N_2S$ (4). The intensity in the high angle region has been multiplied by a factor 10.

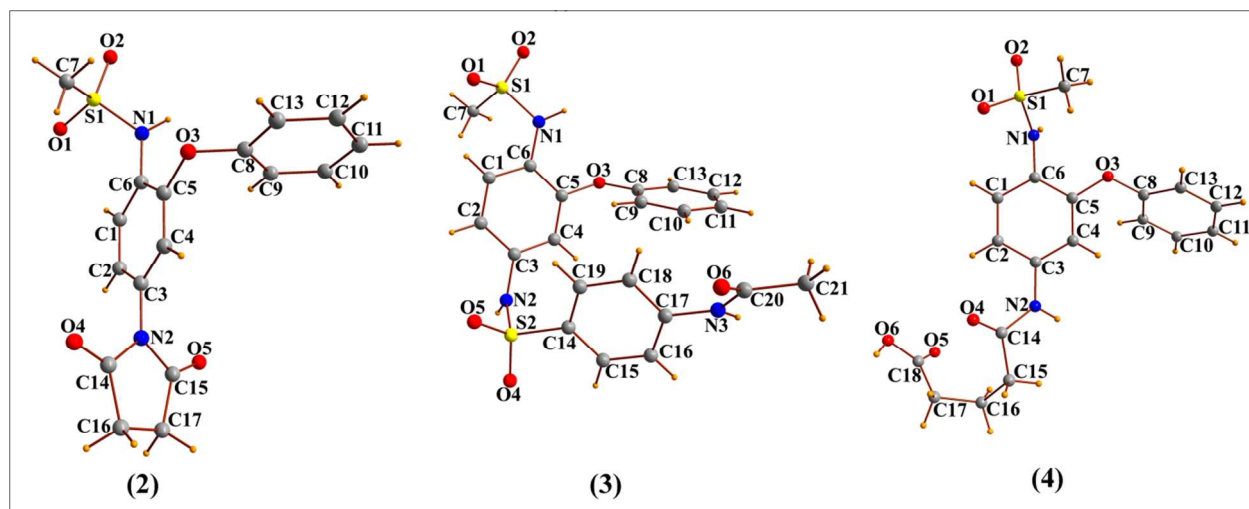


Fig. 2: Molecular views with atom labeling scheme for $C_{17}H_{16}O_5N_2S$ (**2**), $C_{21}H_{21}O_6N_3S_2$ (**3**) and $C_{18}H_{20}O_6N_2S$ (**4**).

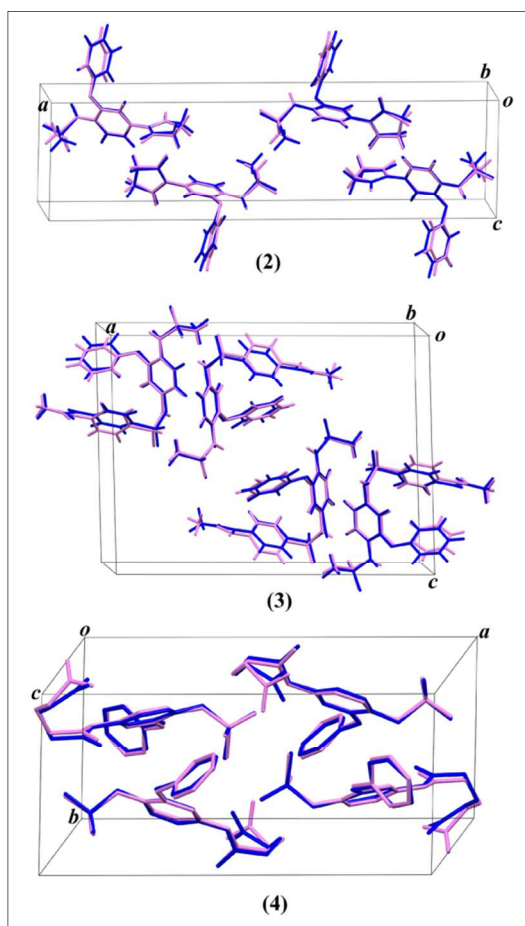


Fig. 3: Superposition of molecular conformations as obtained from X-ray structure analysis (violet) and solid state DFT calculation (blue) for $C_{17}H_{16}O_5N_2S$ (**2**), $C_{21}H_{21}O_6N_3S_2$ (**3**) and $C_{18}H_{20}O_6N_2S$ (**4**). Hydrogen atoms of **4** have been omitted for clarity.

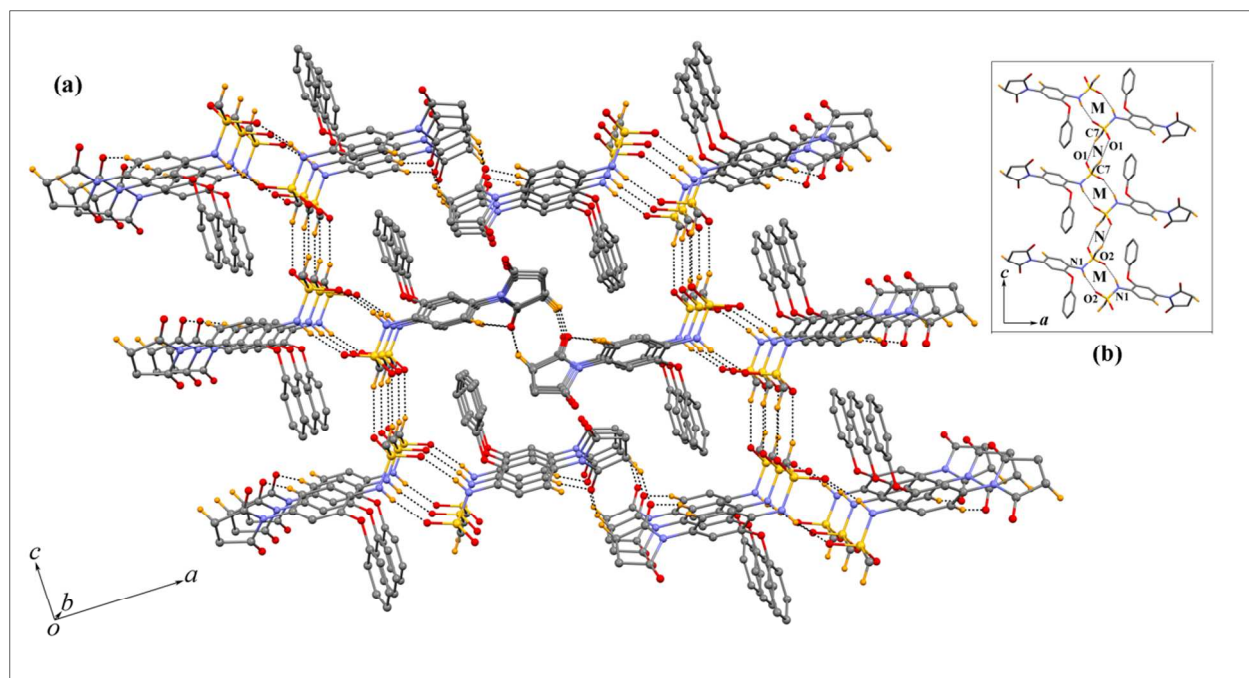


Fig. 4: (a) Three dimensional architecture (b) polymeric MNMN... chain formed by N-H...O and C-H...O hydrogen bonds in $C_{17}H_{16}O_5N_2S$ (**2**).

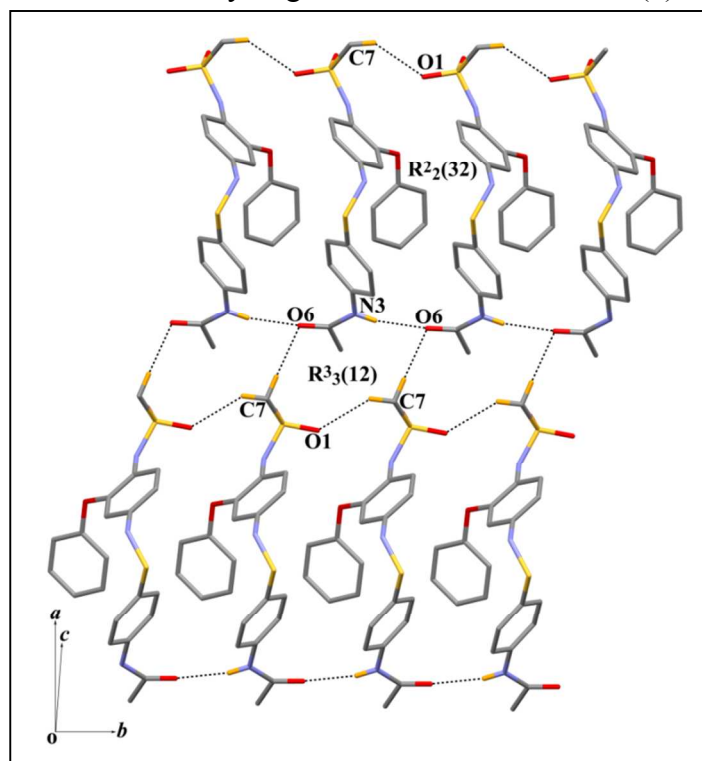


Fig. 5: Two dimensional network formed by N-H...O and C-H...O hydrogen bonds in $C_{21}H_{21}O_6N_3S_2$ (**3**).

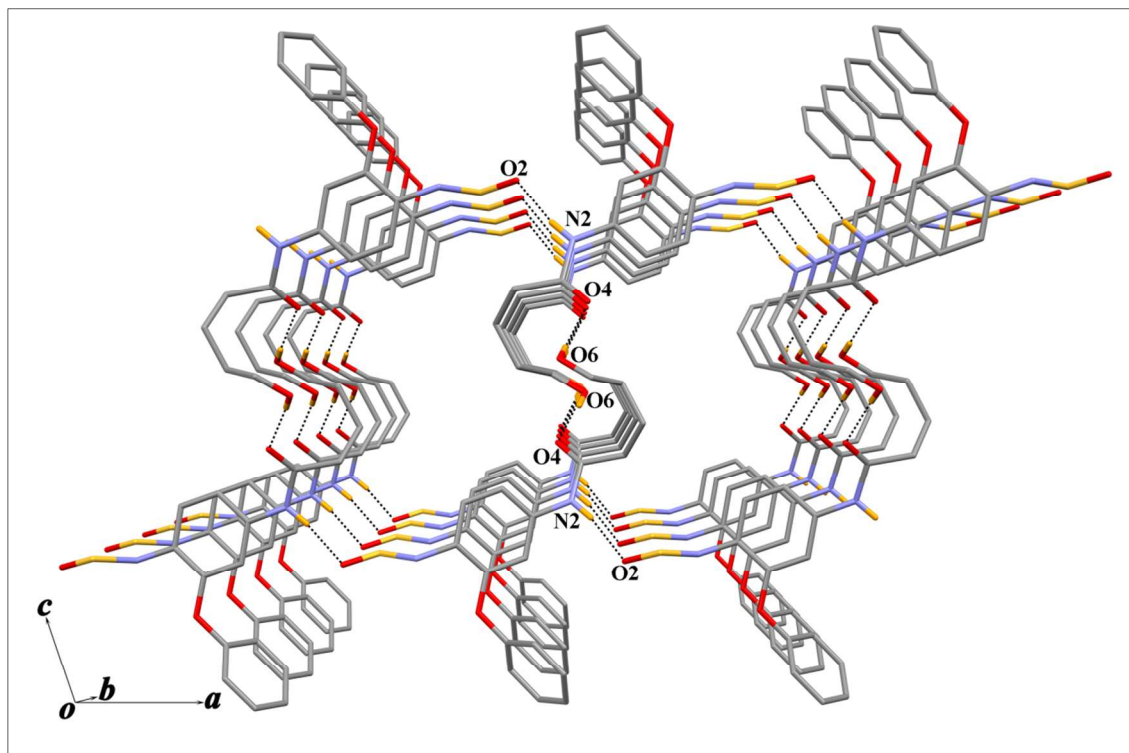


Fig. 6: Two dimensional columnar framework by O-H...O and N-H...O hydrogen bonds in $C_{18}H_{20}O_6N_2S$ (4).

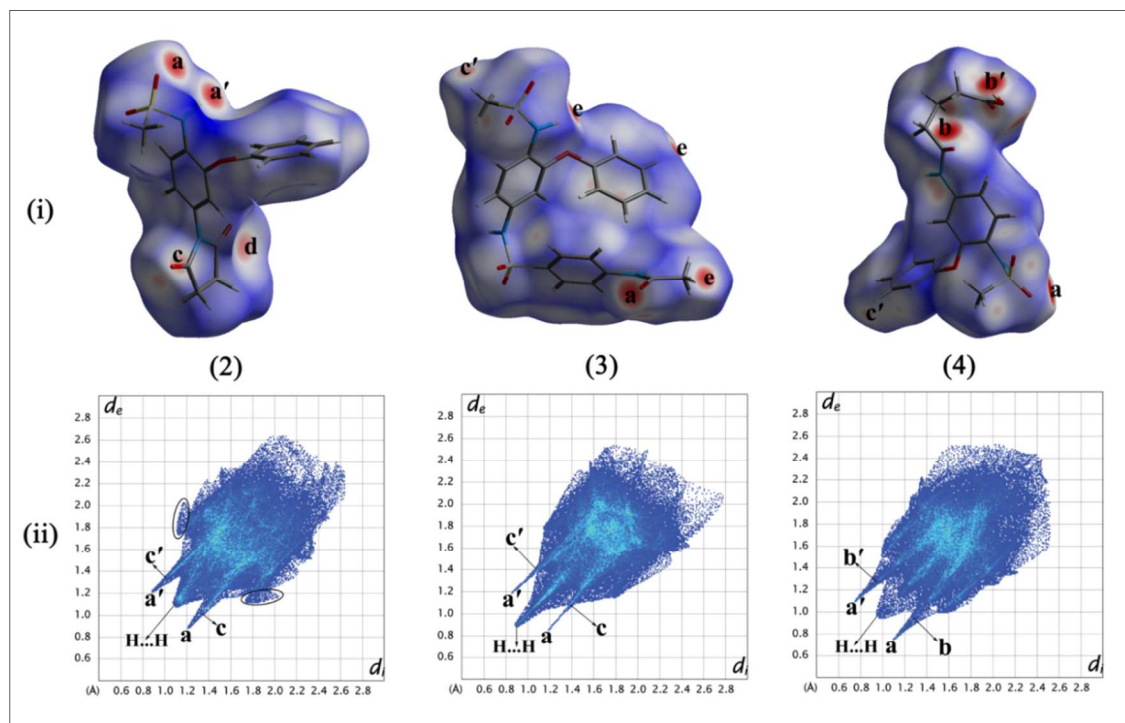


Fig. 7: (i) Hirshfeld surfaces and (ii) fingerprint plots for $C_{17}H_{16}O_5N_2S$ (2), $C_{21}H_{21}O_6N_3S_2$ (3) and $C_{18}H_{20}O_6N_2S$ (4).

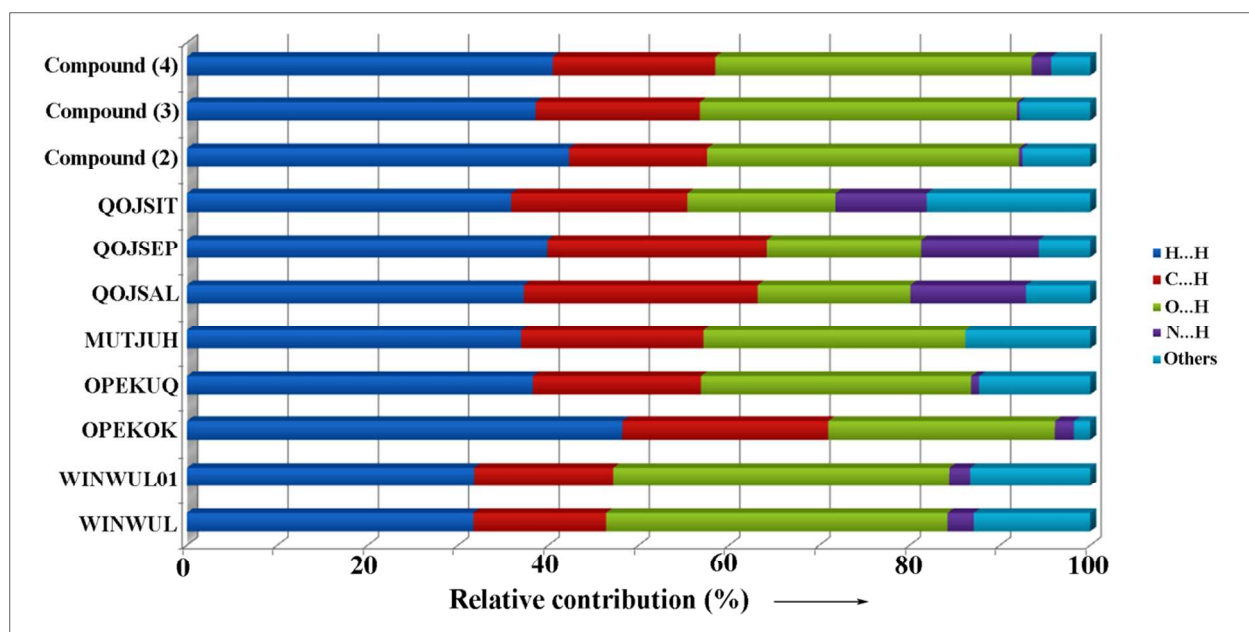


Fig. 8: Relative contribution of different interactions to the Hirshfeld surfaces of $C_{17}H_{16}O_5N_2S$ (2), $C_{21}H_{21}O_6N_3S_2$ (3) and $C_{18}H_{20}O_6N_2S$ (4), and a few related structures from the CSD.

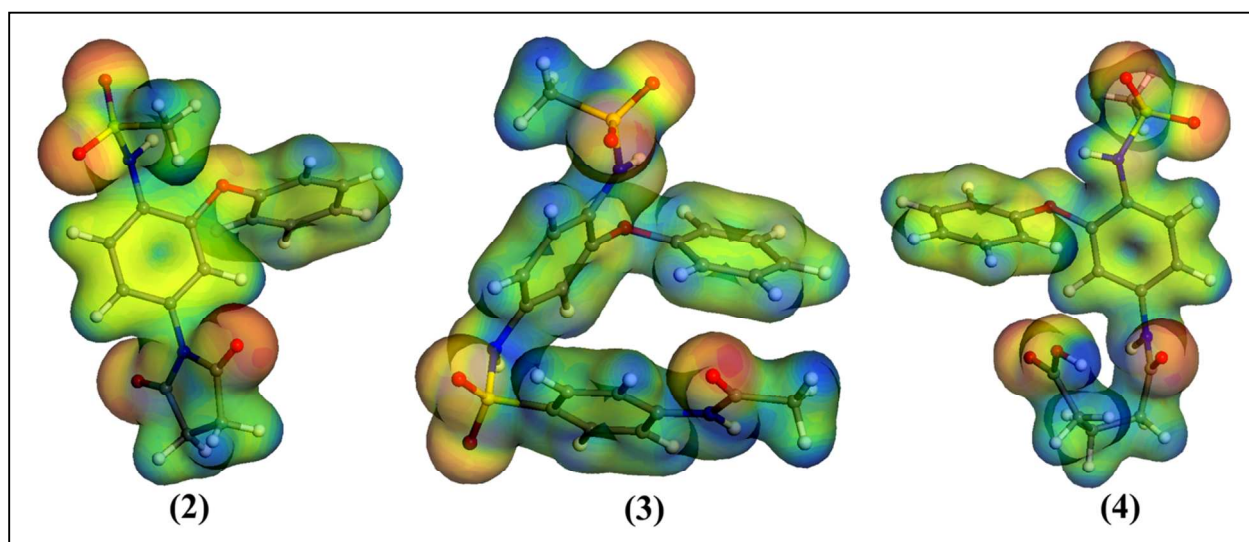


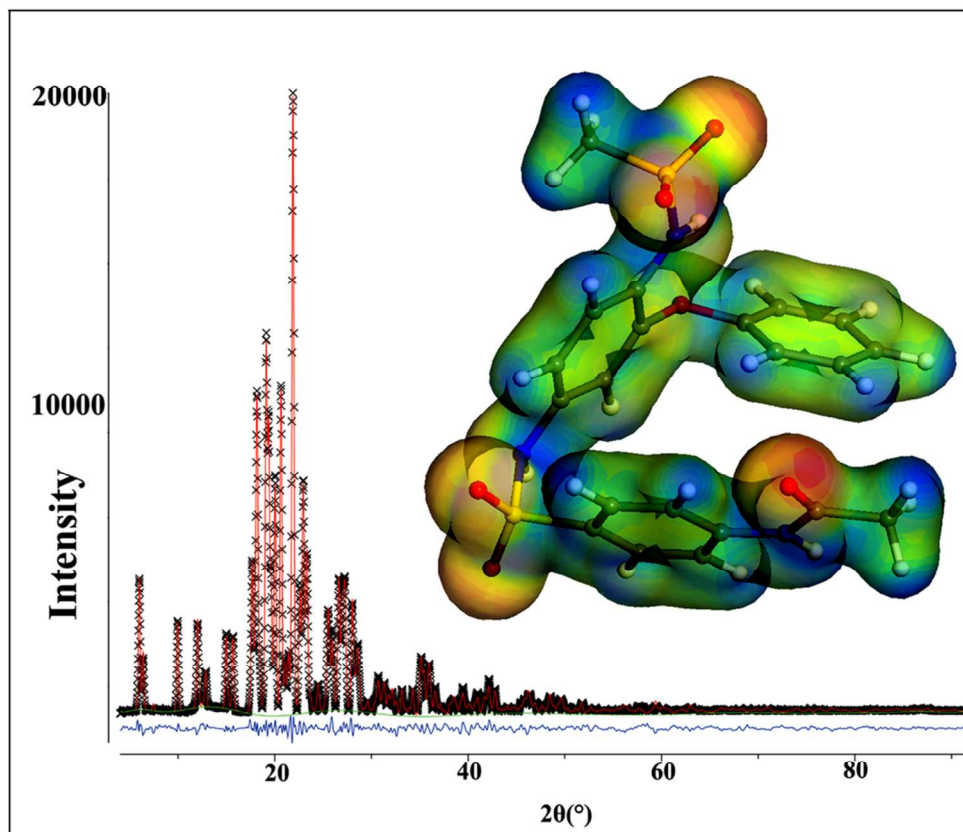
Fig. 9: MEP surfaces of $C_{17}H_{16}O_5N_2S$ (2), $C_{21}H_{21}O_6N_3S_2$ (3) and $C_{18}H_{20}O_6N_2S$ (4).

For Table of Contents Use Only

Three Nimesulide Derivatives: Synthesis, Ab-initio Structure Determination from Powder X-ray Diffraction and Quantitative Analysis of Molecular Surface Electrostatic Potential

Tanusri Dey^a, Paramita Chatterjee^{a,b}, Abir Bhattacharya^c, Sarbani Pal^d and Alok K. Mukherjee^{a,*}

Three nimesulide derivatives have been synthesized, and their crystal structures are determined from X-ray powder diffraction. The nature of intermolecular interactions and relative hydrogen-bond donor strengths has been analyzed through Hirshfeld surface analysis and molecular electrostatic potential surface calculation.



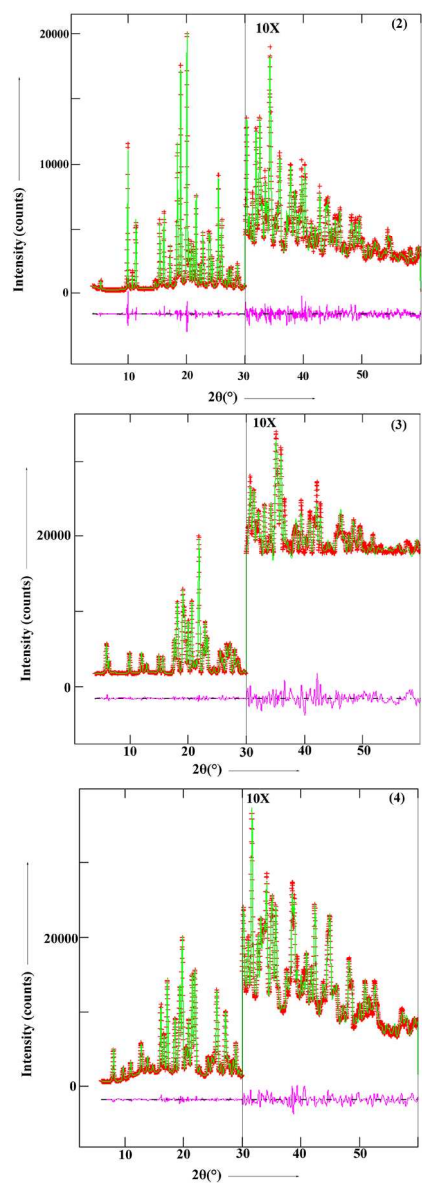


Fig. 1: Final rietveld plot for C₁₇H₁₆O₅N₂S (2), C₂₁H₂₁O₆N₃S₂ (3) and C₁₈H₂₀O₆N₂S (4). The intensity in the high angle region has been multiplied by a factor 10.
235x659mm (300 x 300 DPI)

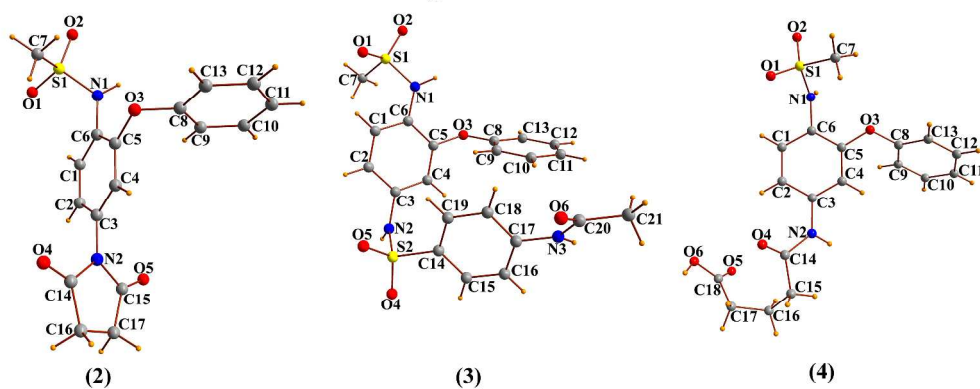


Fig. 2: Molecular views with atom labeling scheme for C17H16O5N2S (2), C21H21O6N3S2 (3) and C18H20O6N2S (4).
438x177mm (300 x 300 DPI)

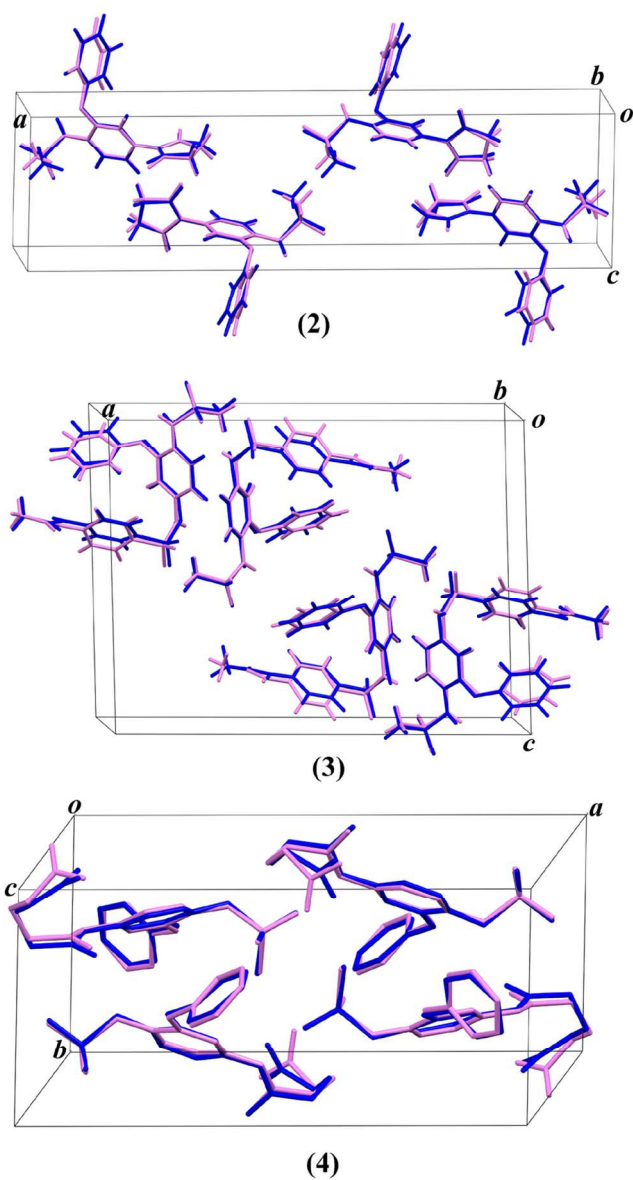


Fig. 3: Superposition of molecular conformations as obtained from X-ray structure analysis (violet) and solid state DFT calculation (blue) for $C_{17}H_{16}O_5N_2S$ (2), $C_{21}H_{21}O_6N_3S_2$ (3) and $C_{18}H_{20}O_6N_2S$ (4). Hydrogen atoms of 4 have been omitted for clarity.
83x146mm (300 x 300 DPI)

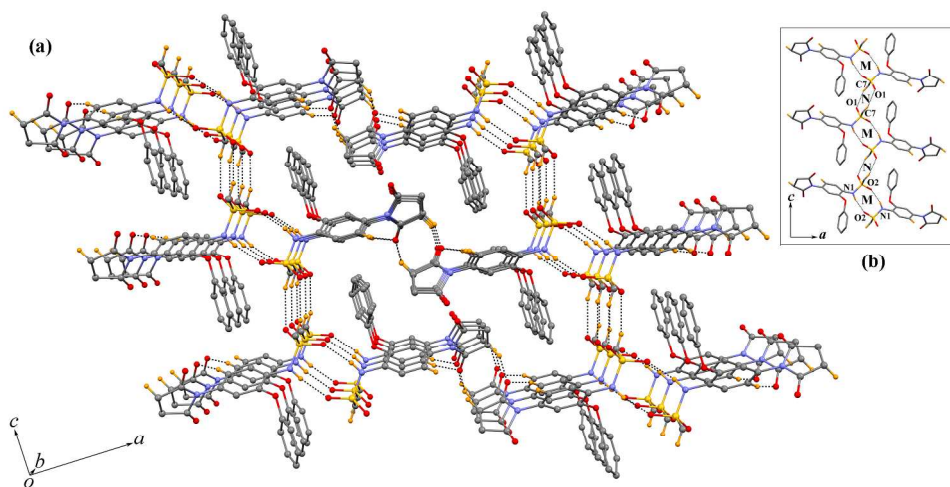


Fig. 4: (a) Three dimensional architecture (b) polymeric MNMN... chain formed by N-H...O and C-H...O hydrogen bonds in C₁₇H₁₆O₅N₂S (2).
254x136mm (300 x 300 DPI)

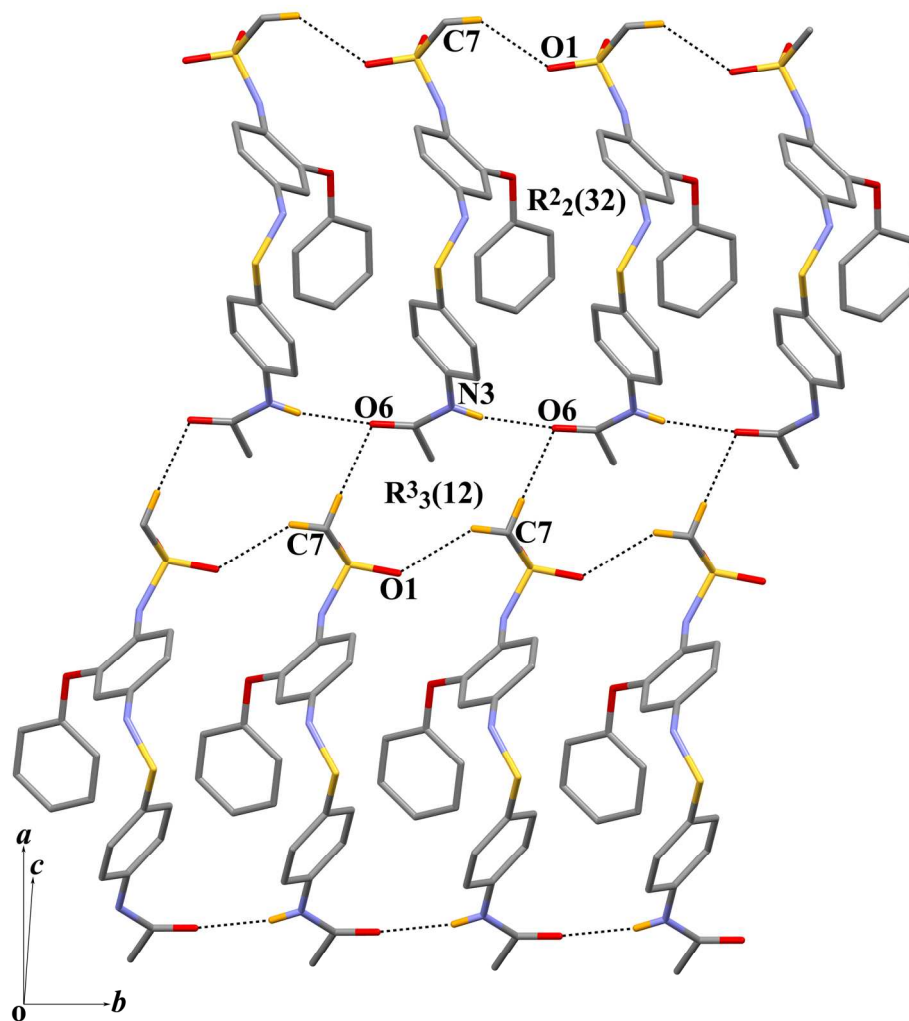


Fig. 5: Two dimensional network formed by N-H...O and C-H...O hydrogen bonds in C₂₁H₂₁O₆N₃S₂ (3).
169x182mm (300 x 300 DPI)

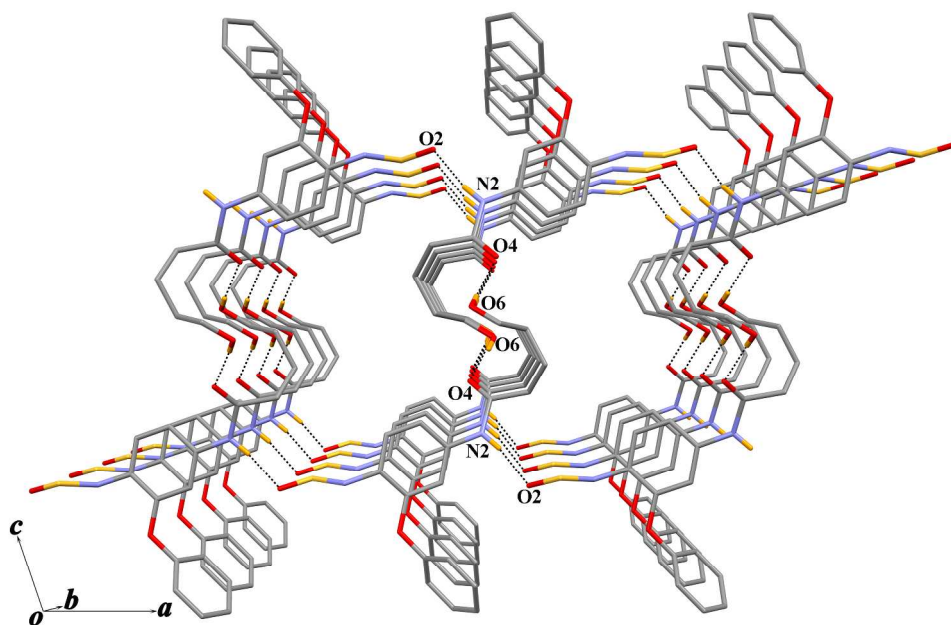


Fig. 6: Two dimensional columnar framework by O-H...O and N-H...O hydrogen bonds in C₁₈H₂₀O₆N₂S (4).
254x168mm (300 x 300 DPI)

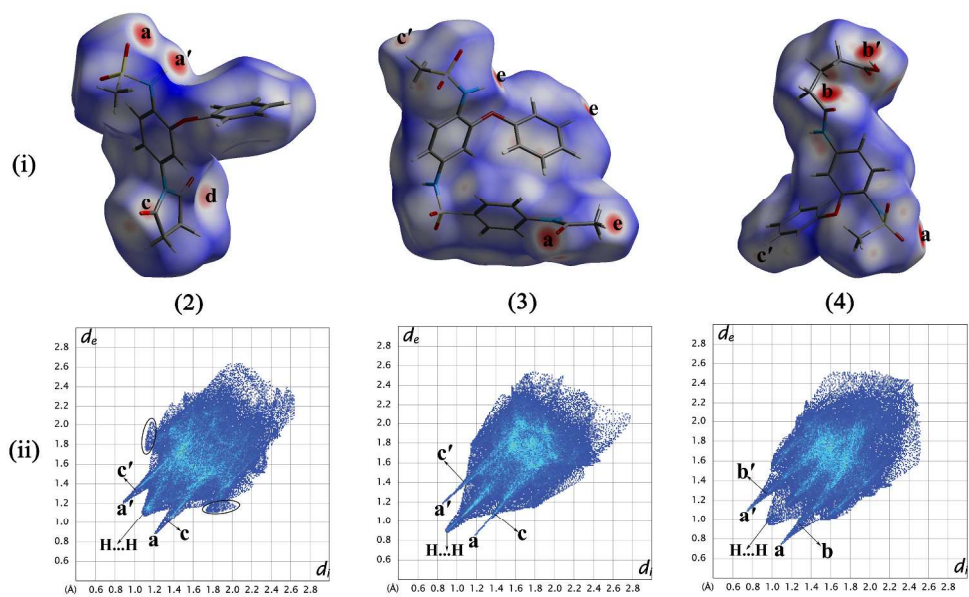


Fig. 7: (i) Hirshfeld surfaces and (ii) fingerprint plots for C₁₇H₁₆O₅N₂S (2), C₂₁H₂₁O₆N₃S₂ (3) and C₁₈H₂₀O₆N₂S (4).
338x216mm (300 x 300 DPI)

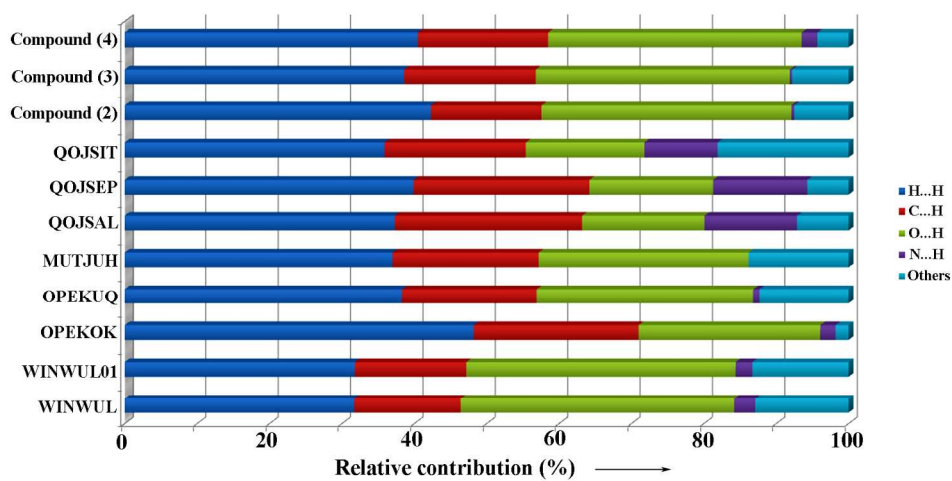


Fig. 8: Relative contribution of different interactions to the Hirshfeld surfaces of C₁₇H₁₆O₅N₂S (2), C₂₁H₂₁O₆N₃S₂ (3) and C₁₈H₂₀O₆N₂S (4), and a few related structures from the CSD.
169x84mm (300 x 300 DPI)

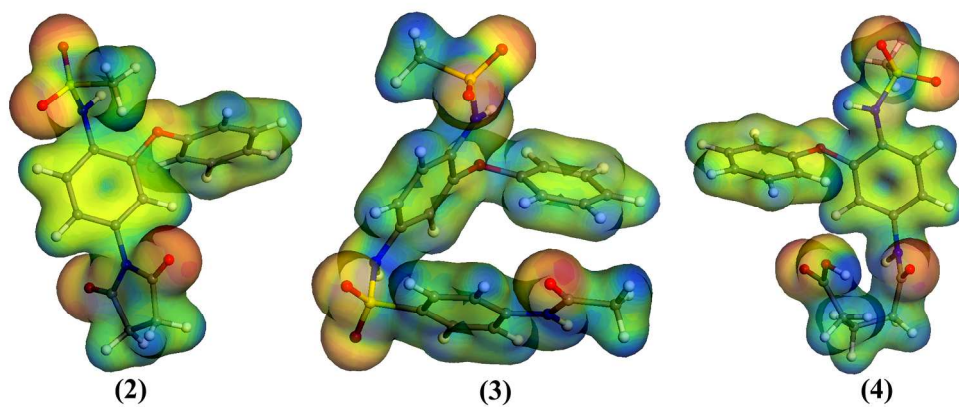
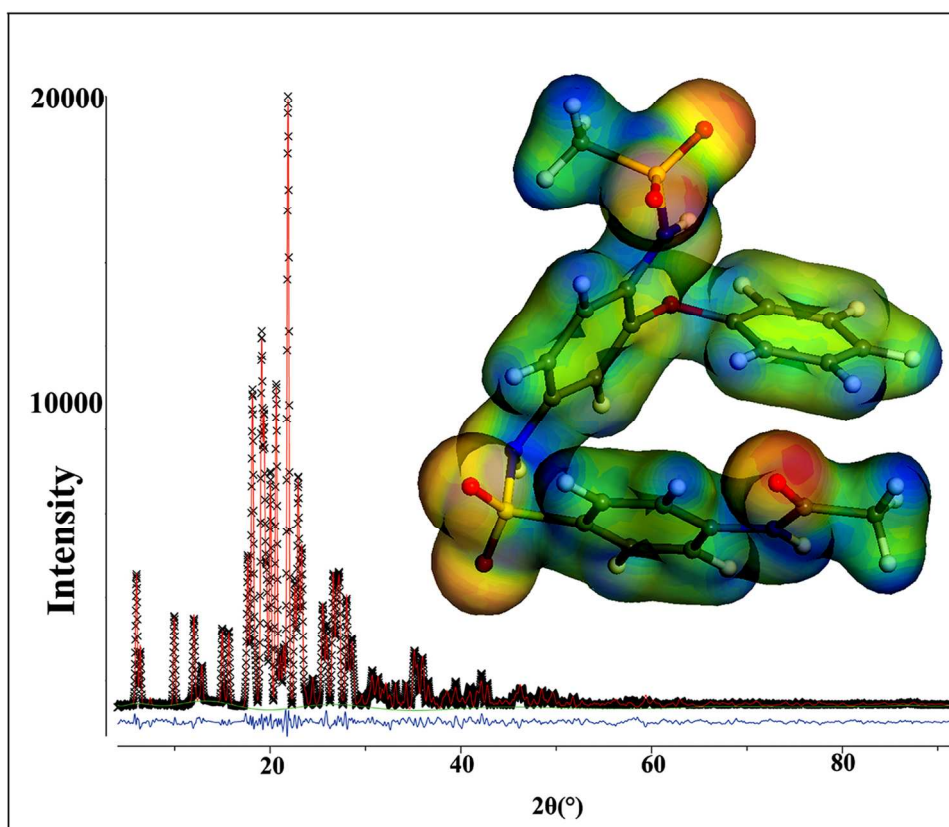


Fig. 9: MEP surfaces of C₁₇H₁₆O₅N₂S (2), C₂₁H₂₁O₆N₃S₂ (3) and C₁₈H₂₀O₆N₂S (4).
211x90mm (300 x 300 DPI)



graphical abstract
134x114mm (300 x 300 DPI)